

Synthesis and Structural Characterization of Sialic Acid-Glutamic Acid Hybrid Foldamers as Conformational Surrogates of α -2,8-Linked Polysialic Acid

Jonel P. Saludes, James B. Ames and Jacquelyn Gervay-Hague*

Department of Chemistry, University of California, One Shields Ave., Davis, CA 95616

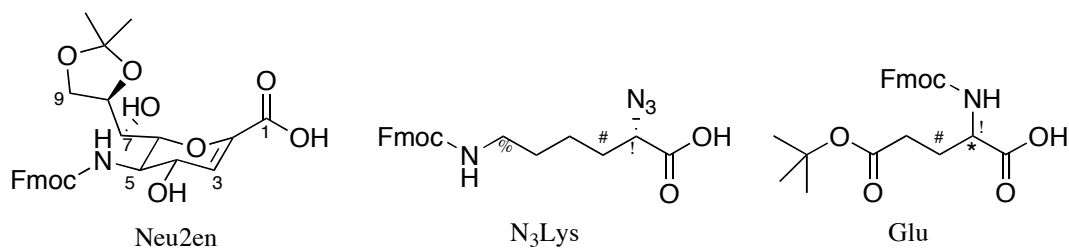
Supporting Information

- S4** Scheme S1: Synthetic scheme for **1**
- S4** Scheme S2: Synthetic scheme for **4**
- S5** Scheme S3: Representative microwave-assisted solid phase peptide synthesis
- S6-S12** Characterization of compounds **5-11**
- S13-S14** Figure S1: Mass spectra of compounds **5-12**
- S15** Figure S2: ^1H NMR spectrum of compound **5**
- S16** Figure S3: ^1H NMR spectrum of compound **6**
- S17** Figure S4: ^1H NMR spectrum of compound **7**
- S18** Figure S5: ^1H NMR spectrum of compound **8**
- S19** Figure S6: ^1H NMR spectrum of compound **9**
- S20** Figure S7: ^1H NMR spectrum of compound **10**
- S21** Figure S8: ^1H NMR spectrum of compound **11**
- S22** Figure S9: ^1H NMR spectrum of compound **12**
- S23** Figure S10: ^{13}C NMR spectrum of compound **5**
- S24** Figure S11: ^{13}C NMR spectrum of compound **6**
- S25** Figure S12: ^{13}C NMR spectrum of compound **7**
- S26** Figure S13: ^{13}C NMR spectrum of compound **8**
- S27** Figure S14: ^{13}C NMR spectrum of compound **9**

- S28** Figure S15: ^{13}C NMR spectrum of compound **10**
- S29** Figure S16: ^{13}C NMR spectrum of compound **11**
- S30** Figure S17: ^{13}C NMR spectrum of compound **12**
- S31** Figure S18: Stack plot of the amide regions from the ^1H NMR DMSO- d_6 at 298 K, 600 MHz of **6**, **8**, **10**, and **12**
- S32** Figure S19: NH/ND exchange study for **6**, **8**, **10**, and **12** in DMSO- d_6 at 298 K, 600 MHz.
- S33** Figure S20: Sample IR spectra and plots of amide/azide peak area integration used to monitor SPPS
- S34** Assignment strategy for the NMR chemical shifts of **11** and **12**.
- S37** Figure S21: Prominent long range ROE's for **12**
- S38** Figure S22. The effect of solvent and solvent screening of electrostatic charges in the X-PLOR structure calculation
- S39** Table 1: ROEs observed in the 500 ms ROESY spectrum of **10** in 9:1 $\text{H}_2\text{O}/\text{D}_2\text{O}$ at 600 MHz, 298 K.
- S40** Table 2: ROEs observed in the 500 ms ROESY spectrum of **12** in 9:1 $\text{H}_2\text{O}/\text{D}_2\text{O}$ at 600 MHz, 298 K.
- S41** Figure S23: Overlay of 25 low energy structures of **8** showing non-convergence to a single-preferred structure
- S42** Figure S24: UV spectrum of **6** in D_2O .
- S42** Figure S23: UV spectrum of **8** in D_2O .
- S43** Figure S26: UV spectrum of **10** in D_2O .
- S44** Figure S27: UV spectrum of **12** in D_2O .

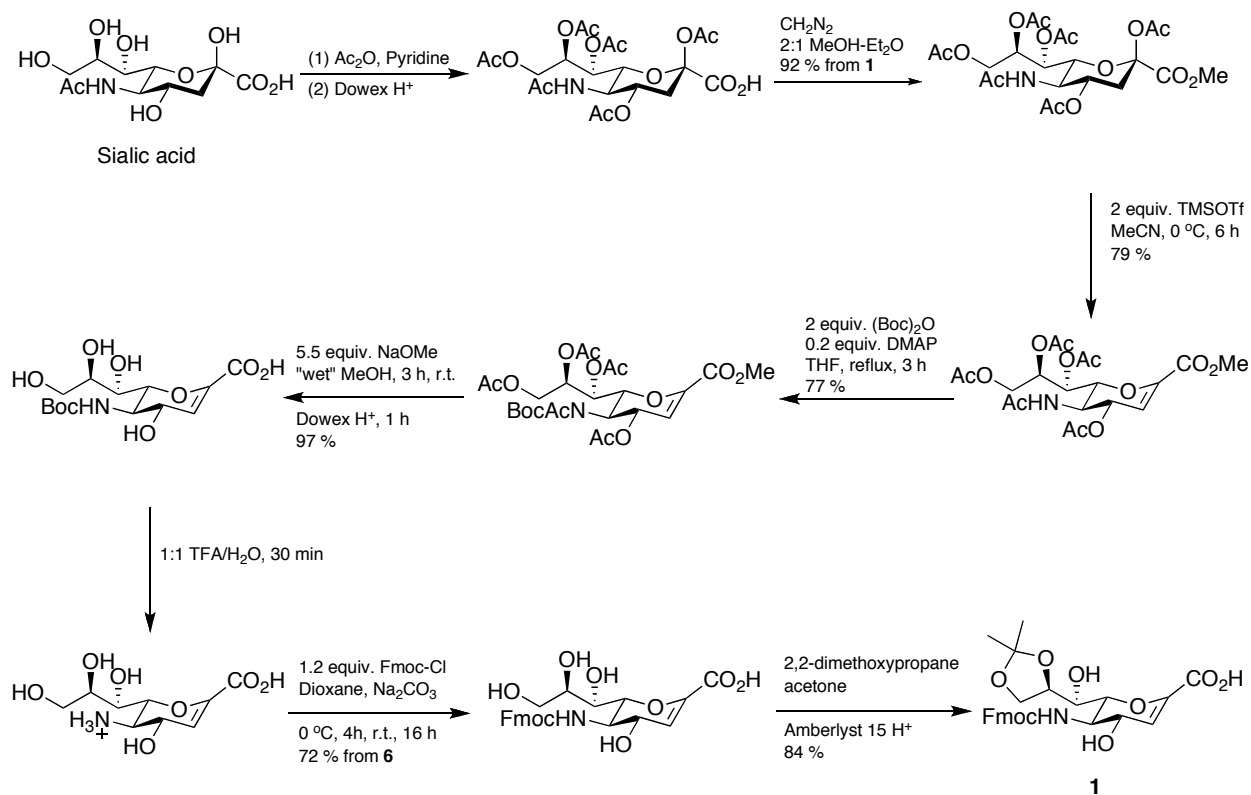
General Experimental Section. NMR spectra were recorded on 400 and 600 MHz NMR spectrometers. Chemical shifts were referenced to residual CHCl_3 ($\delta_{\text{H}} = 7.26$), CHD_2OD ($\delta_{\text{H}} = 3.30$), $(\text{CHD}_2)_2\text{CO}$ ($\delta_{\text{H}} = 2.05$), CDCl_3 ($\delta_{\text{C}} = 77.1$), CD_3OD , ($\delta_{\text{C}} = 49.0$) or $(\text{CD}_3)_2\text{CO}$ ($\delta_{\text{C}} = 39.0$). Solutions in D_2O were referenced to dioxane calibrated to TSP. Low-resolution mass spectra were obtained using a QTRAP mass spectrometer. High Resolution mass spectra were recorded at the UC Davis Molecular Structure Facility using MALDI-TOF with internal calibration. Infrared spectra were recorded on an ATR-FTIR spectrometer. Microwave-assisted SPPS was done using a commercial microwave reactor. Rink amide resin, *N*-acetylneuraminic acid, and Fmoc-Glu(OBt)-OH, and *N*-acetylneuraminic acid were obtained from commercial sources. Reagents were used as received unless otherwise indicated. Solution phase reactions were monitored by TLC using Si gel 60 F254 or RP- C_{18} glass-backed plate.

Amino acids used for constructing the α/δ hybrid peptides



Synthesis of Sialic Acid Derivative Fmoc-Neu2en (**1**)

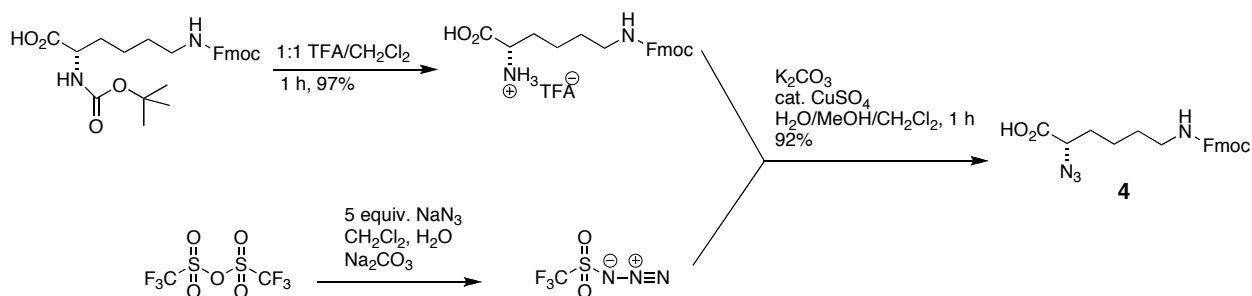
N-(9-fluorenylmethoxycarbonyl)-2,3-dehydro-8,9-isopropylidene neuraminic acid **1** (Fmoc-Neu2en) was synthesized following our previous method¹ with slight modification to furnish an overall yield of 32% in eight steps Scheme 1.



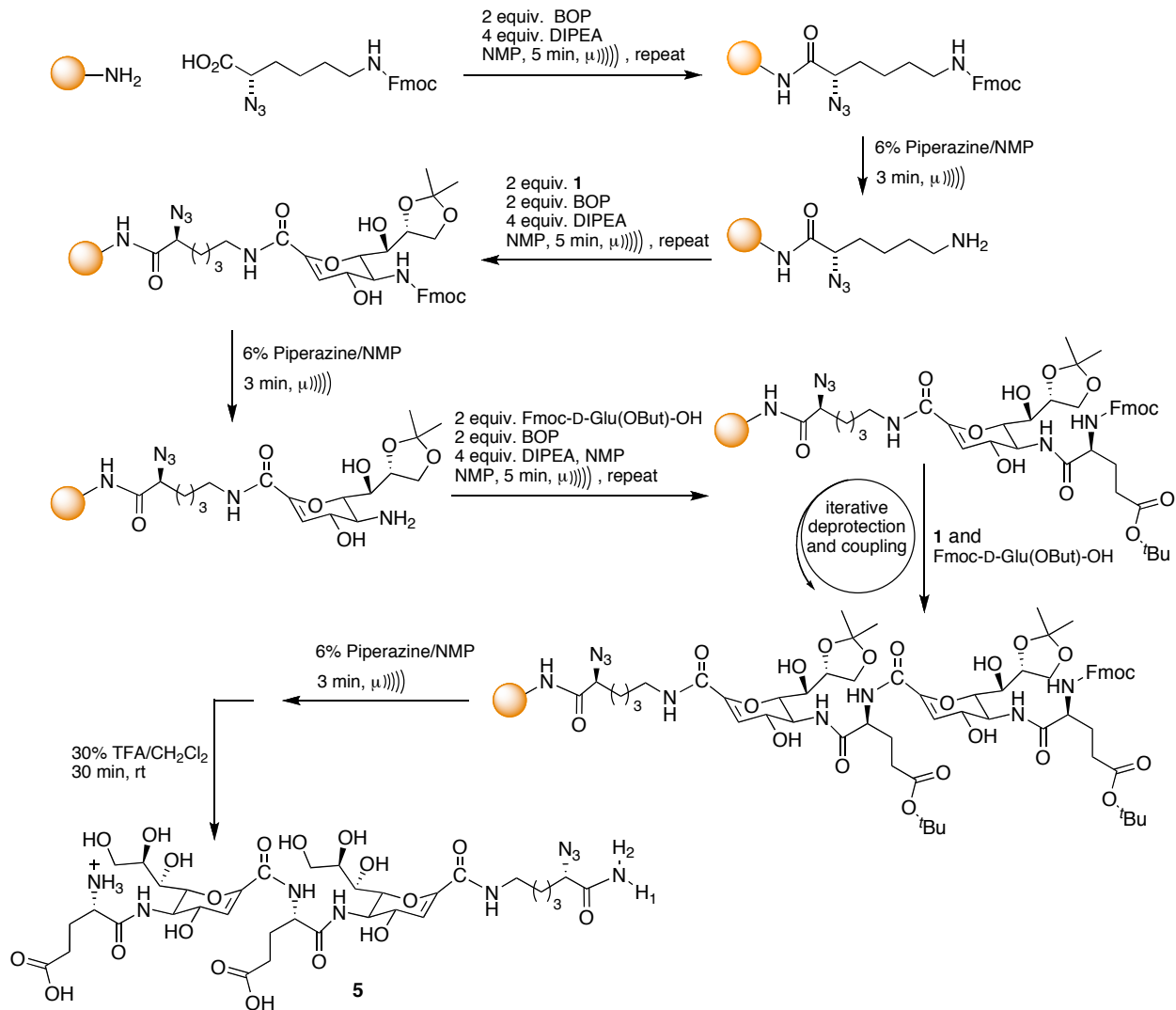
Scheme S1. Synthetic scheme for **1**.

Synthesis of Azidolysine Linker (**4**)

Compound **4** (N₃Lys) was prepared following the method developed by Wong,² and adopted by others.³ The crude product was concentrated to dryness, and chromatographed through a column of silica gel using 85:15 CH₂Cl₂-MeOH to yield **4** (2.07 g, 92%) as shown in Scheme 2.

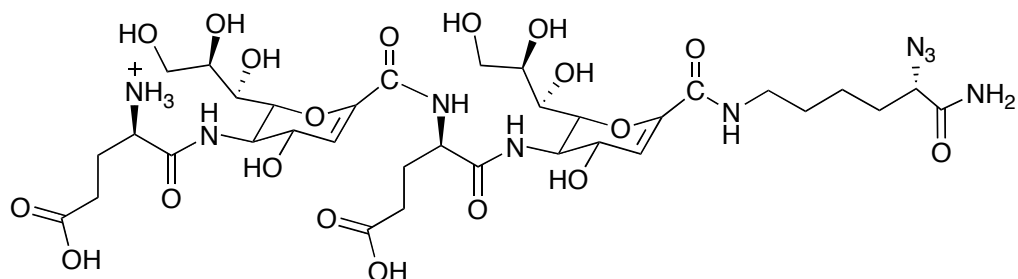


Scheme S2. Synthetic scheme for **4**.

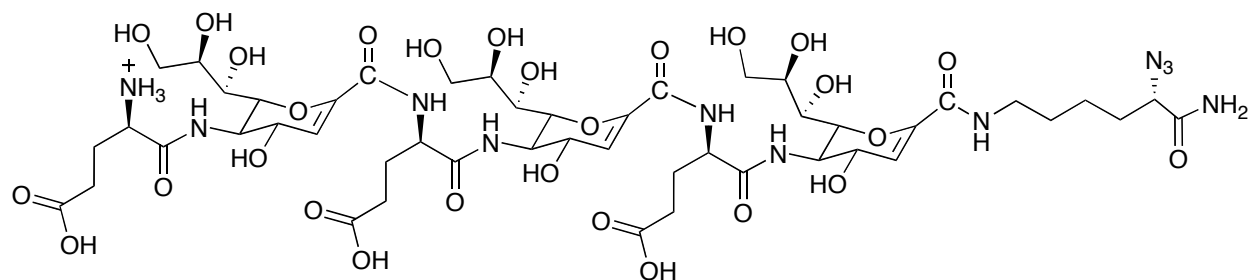


Scheme S3. Representative microwave-assisted solid phase peptide synthesis.

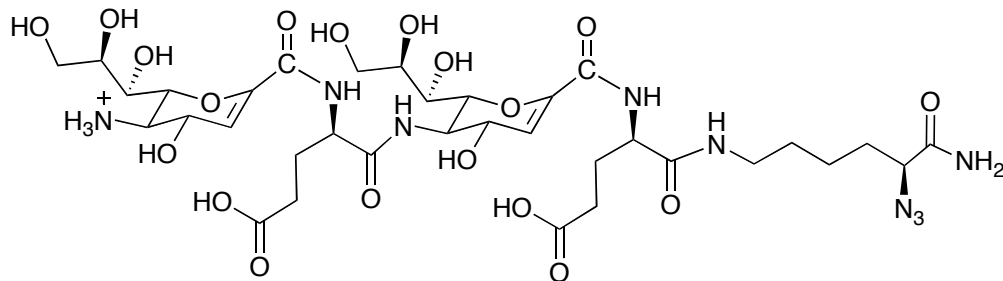
Assignments of H for each oligomer are based upon the following system: **HX-Y**, which refers to **H** in position **X** at residue number **Y** counting from the *N*-terminus.



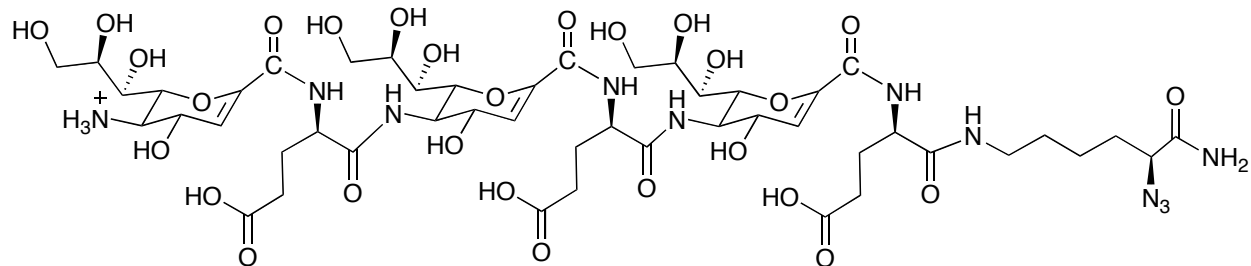
Neu2en/D-Glu-4 (5): obtained in 27% purified yield. ^1H NMR (D_2O , 600 MHz): d 5.91 (d, 1H, $J = 3.0$ Hz, H3-2), 5.82 (d, 1H, $J = 3.0$ Hz, H3-4), 4.57 (dd, 1H, $J = 7.2, 2.4$ Hz, H4-2), 4.55 (dd, 1H, $J = 7.2, 2.4$ Hz, H3-4), 4.54 (dd, 1H, $J = 7.2, 4.8$ Hz, H α -3), 4.48 (dd, 1H, $J = 10.8, 0.6$ Hz, H6-2), 4.39 (dd, 1H, $J = 10.8, 0.6$ Hz, H6-4), 4.24 (dd, 1H, $J = 10.8, 9.0$ Hz, H5-2), 4.16 (dd, 1H, $J = 10.8, 8.4$ Hz, H5-2), 4.15 (dd, 1H, $J = 4.8, 2.4$ Hz, H α -5), 4.14 (dd, 1H, $J = 4.8, 2.4$ Hz, H α -2), 4.00 (ddd, 1H, $J = 9.6, 5.4, 2.4$ Hz, H8-2), 3.92-3.88 (m, 3H, H8-4, H9/9'-2), 3.71 (dd, 1H, $J = 6.0, 6.0$ Hz, H9'-4), 3.69 (dd, 1H, $J = 3.0, 3.0$ Hz, H7-2), 3.67 (dd, 1H, $J = 6.0, 6.0$ Hz, H9-4), 3.62 (d, 1H, $J = 9.0$ Hz, H7-4), 3.37-3.28 (m, 2H, H ϵ -5), 2.62-2.49 (m, 4H, H γ -1/3), 2.28-2.09 (m, 4H, H β -1/3), 1.90-1.78 (m, 2H, H β -5), 1.66-1.58 (m, 2H, H δ -5), 1.44 (p, 2H, $J = 7.8$ Hz, H γ -5). ^{13}C NMR (D_2O , 150 MHz): d 180.2, 179.3, 178.3, 176.2, 172.8, 166.4, 148.7, 148.0, 111.7, 110.9, 78.8, 72.7, 70.7, 70.2, 69.8, 65.8, 65.7, 56.5, 55.9, 55.8, 52.8, 42.0, 33.6, 33.1, 32.6, 30.6, 29.1, 24.8. MALDI-TOFMS: $[\text{M} + \text{Na}^+]$ calcd for $\text{C}_{34}\text{H}_{53}\text{N}_9\text{O}_{19}\text{Na}^+$, 914.3350; found, 914.3400.



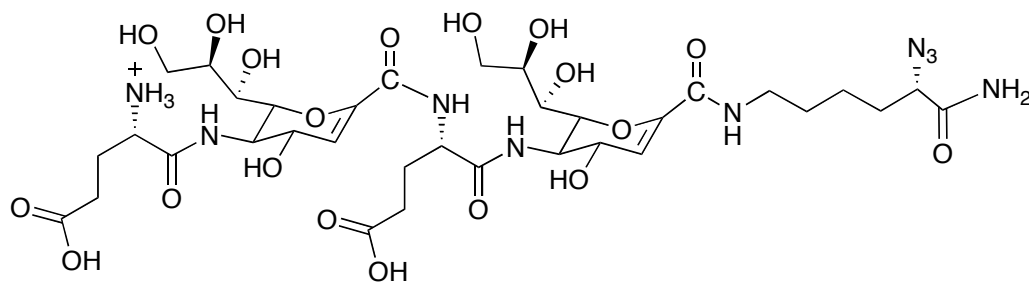
Neu2en/D-Glu-6 (6): obtained in 39% purified yield. ^1H NMR (D_2O , 600 MHz): d 5.91 (d, 1H, $J = 2.4$ Hz, H3-2), 5.89 (d, 1H, $J = 2.4$ Hz, H3-4), 5.82 (d, 1H, $J = 1.8$ Hz, H3-6), 4.57-4.51 (m, 5H, H4-6, H α -5, H4-4, H α -3, H4-2), 4.48 (dd, 1H, $J = 10.8, 1.2$ Hz, H6-2), 4.43 (dd, 1H, $J = 10.8, 1.2$ Hz, H6-4), 4.38 (dd, 1H, $J = 10.8, 1.2$ Hz, H6-6), 4.24 (dd, 1H, $J = 10.8, 9.0$ Hz, H5-2), 4.20-4.18 (m, 1H, H5-4), 4.15 (dd, 1H, $J = 9.0, 1.8$ Hz, H5-6), 4.14 (t, 1H, $J = 5.4$ Hz, H α -7), 4.14-4.12 (m, 1H, H α -1), 4.01-3.96 (m, 3H, H8-2/4), 3.91-3.85 (m, 5H, H8-6, H9-2/4), 3.72-3.61 (m, 5H, H7-6, H9-6, H7-4, H7-2), 3.37-3.28 (m, 2H, H ϵ -7), 2.58-2.47 (m, 6H, H γ -1/3/5), 2.27-2.09 (m, 6H, H β -1/3/5), 1.88-1.78 (m, 2H, H β -7), 1.61 (p, 2H, $J = 6.6$ Hz, H δ -7), 1.44 (p, 2H, $J = 7.8$ Hz, H γ -7). ^{13}C NMR (D_2O , 150 MHz): d 180.7, 180.4, 179.9, 178.4, 176.5, 172.7, 166.6, 166.0, 148.6, 148.0, 111.9, 111.7, 110.9, 79.0, 78.9, 72.9, 72.8, 70.8, 70.7, 69.7, 69.6, 65.9, 65.8, 65.7, 56.6, 55.8, 52.9, 52.8, 41.9, 33.8, 33.4, 33.0, 30.7, 29.4, 29.3, 24.8. MALDI-TOFMS: $[\text{M} + \text{Na}^+]$ calcd for $\text{C}_{48}\text{H}_{73}\text{N}_{11}\text{O}_{28}\text{Na}^+$, 1274.4518; found, 1274.452.



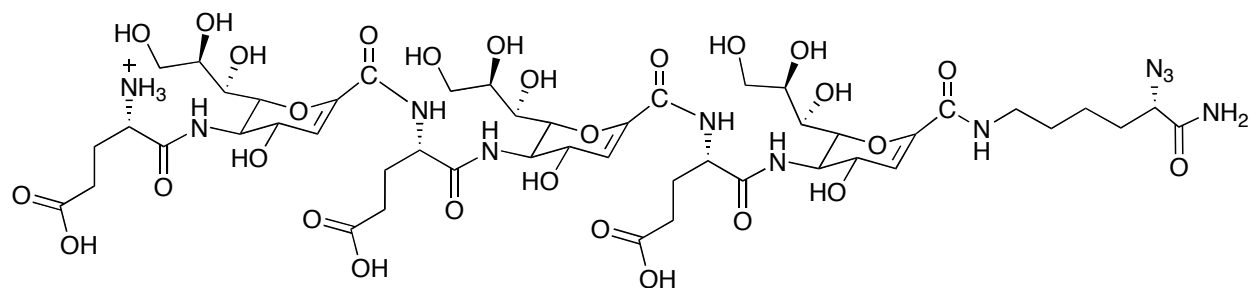
D-Glu/Neu2en-4 (7): obtained in 39% purified yield. ^1H NMR (D_2O , 600 MHz): d 5.97 (d, 1H, $J = 2.4$ Hz, H3-1), 5.90 (d, 1H, $J = 2.4$ Hz, H3-3), 4.66 (dd, 1H, $J = 8.4, 3.0$ Hz, H4-1), 4.65 (dd, 1H, $J = 10.2, 1.8$ Hz, H6-1), 4.58 (dd, 2H, $J = 9.0, 2.4$ Hz, H4-3, H α -2), 4.45 (dd, 1H, $J = 10.8, 0.6$ Hz, H6-3), 4.43 (dd, 1H, $J = 9.0, 5.4$ Hz, H α -4), 4.20 (dd, 1H, $J = 10.8, 9.0$ Hz, H5-3), 4.15 (dd, 1H, $J = 7.2, 5.4$ Hz, H α -5), 4.08 (ddd, 1H, $J = 9.0, 5.4, 2.4$ Hz, H8-1), 4.00 (ddd, 1H, $J = 9.6, 6.0, 2.4$ Hz, H8-3), 3.94 (dd, 1H, $J = 12.0, 2.4$ Hz, H9'-1), 3.92 (dd, 1H, $J = 10.8, 2.4$ Hz, H7-1), 3.91 (dd, 1H, $J = 9.0, 1.8$ Hz, H9-3), 3.71 (dd, 1H, $J = 12.0, 6.0$ Hz, H9'-3), 3.66 (dd, 1H, $J = 9.6, 1.2$ Hz, H7-3), 3.65 (dd, 1H, $J = 10.2, 8.4$ Hz, H5-1), 3.31-3.22 (m, 2H, H ϵ -5), 2.60-2.48 (m, 4H, H γ -2/4), 2.30-2.06 (m, 4H, H β -2/4), 1.91-1.77 (m, 2H, H β -5), 1.64-1.52 (m, 2H, H δ -5), 1.44 (p, 2H, $J = 7.2$ Hz, H γ -5). ^{13}C NMR (D_2O , 150 MHz): d 180.3, 180.2, 178.4, 176.3, 175.7, 166.4, 166.0, 145.0, 111.8, 111.0, 79.0, 77.9, 72.9, 72.8, 70.8, 70.6, 69.7, 67.6, 66.0, 65.8, 65.5, 56.6, 56.4, 53.7, 52.9, 41.8, 33.8, 33.1, 30.8, 29.2, 24.8. MALDI-TOFMS: $[\text{M} + \text{Na}^+]$ calcd for $\text{C}_{34}\text{H}_{53}\text{N}_9\text{O}_{19}\text{Na}^+$, 914.3350; found, 914.3410.



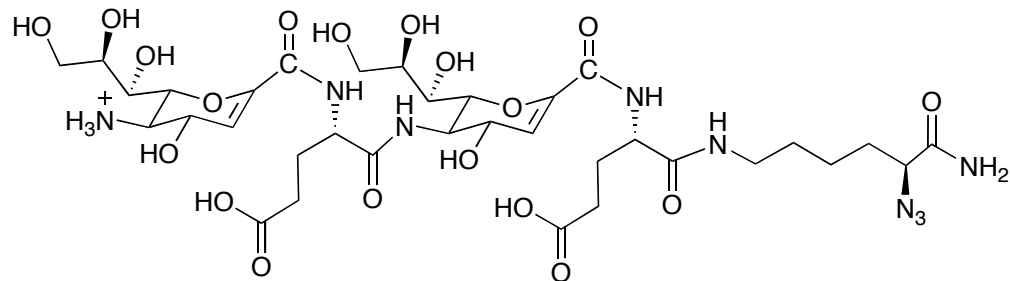
D-Glu/Neu2en-6 (8): obtained in 24% purified yield. ^1H NMR (D_2O , 600 MHz): δ 5.98 (d, 1H, J = 2.4 Hz, H3-1), 5.92 (d, 1H, J = 2.4 Hz, H3-3), 5.90 (d, 1H, J = 2.4 Hz, H3-5), 4.67 (dd, 1H, J = 6.6, 2.4 Hz, H4-1), 4.66 (dd, 1H, J = 7.8, 2.4 Hz, H6-1), 4.59 (dd, 2H, J = 9.0, 2.4 Hz, H4-3/5), 4.58 (dd, 1H, J = 9.0, 4.8 Hz, H α -2), 4.56 (dd, 1H, J = 8.4, 4.2 Hz, H α -4), 4.47 (dd, 1H, J = 7.2, 1.2 Hz, H6-3), 4.45 (dd, 1H, J = 7.2, 1.2 Hz, H6-5), 4.42 (dd, 1H, J = 9.0, 5.4 Hz, H α -6), 4.22 (dd, 1H, J = 9.0, 4.8 Hz, H5-3), 4.20 (dd, 1H, J = 8.4, 4.2 Hz, H5-5), 4.16 (dd, 1H, J = 7.8, 5.4 Hz, H α -7), 4.07 (ddd, 1H, J = 9.0, 5.4, 3.0 Hz, H8-1), 4.03-3.99 (m, 2H, H8-3/5), 3.95 (dd, 1H, J = 12.0, 3.0 Hz, H9'-1), 3.93 (dd, 2H, J = 11.4, 2.4 Hz, H9'-3/5), 3.92 (dd, 1H, J = 8.4, 1.8 Hz, H7-1), 3.80 (dd, 1H, J = 12.6, 6.0 Hz, H9-1), 3.73 (dd, 1H, J = 6.6, 1.8 Hz, H9-3), 3.71 (dd, 1H, J = 7.8, 1.8 Hz, H9-5), 3.67 (dd, 1H, J = 9.0, 1.2 Hz, H7-3), 3.66 (dd, 1H, J = 9.0, 1.2 Hz, H5-5), 3.32-3.22 (m, 2H, H ϵ -7), 2.60-2.49 (m, 6H, H γ -2/4/6), 2.31-2.07 (m, 6H, H β -2/4/6), 1.91-1.78 (m, 2H, H β -7), 1.63-1.56 (m, 2H, H δ -7), 1.44 (p, 2H, J = 7.8 Hz, H γ -7). ^{13}C NMR (D_2O , 150 MHz): δ 180.3, 178.3, 176.2, 175.6, 166.2, 166.1, 165.8, 148.1, 148.0, 111.8, 110.9, 79.0, 77.8, 72.9, 72.6, 70.7, 70.5, 69.6, 67.5, 65.9, 65.8, 65.4, 56.5, 53.7, 52.7, 41.8, 33.7, 33.3, 30.7, 29.3, 24.8. MALDI-TOFMS: $[\text{M} + \text{Na}^+]$ calcd for $\text{C}_{48}\text{H}_{73}\text{N}_{11}\text{O}_{28}\text{Na}^+$, 1274.4518; found, 1274.452.



Neu2en/L-Glu-4 (9): obtained in 28% purified yield. ^1H NMR (D_2O , 600 MHz): d 5.89 (d, 1H, $J = 2.4$ Hz, H3-2), 5.83 (d, 1H, $J = 1.8$ Hz, H3-4), 4.53 (dd, 1H, $J = 9.0, 2.4$ Hz, H4-2), 4.52 (dd, 1H, $J = 9.0, 2.4$ Hz, H4-4), 4.49 (dd, 1H, $J = 9.0, 5.4$ Hz, H α -1), 4.42 (d, 1H, $J = 10.8$ Hz, H6-2), 4.39 (d, 1H, $J = 10.8$ Hz, H6-4), 4.22 (dd, 1H, $J = 10.8, 9.0$ Hz, H5-2), 4.16-4.12 (m, 2H, H α -5, H5-4), 4.11 (m, 1H, H α -3), 4.00 (ddd, 1H, $J = 9.6, 5.4, 2.4$ Hz, H8-2), 3.96-3.86 (m, 2H, H8-4, H9'-2), 3.72 (d, 1H, $J = 10.2$ Hz, H7-2), 3.70-3.69 (m, 2H, H9-2/4), 3.68 (d, 1H, $J = 10.8$ Hz, H7-4), 3.38-3.28 (m, 2H, H ϵ -5), 2.66-2.51 (m, 4H, H γ -1/3), 2.35-2.10 (m, 4H, H β -1/3), 1.89-1.77 (m, 2H, H β -5), 1.65-1.57 (m, 2H, H δ -5), 1.44 (p, 2H, $J = 7.8$ Hz, H γ -5). ^{13}C NMR (D_2O , 150 MHz): d 180.0, 179.0, 178.1, 176.2, 172.4, 166.3, 166.1, 148.2, 147.6, 111.8, 110.8, 78.9, 72.7, 72.5, 70.6, 70.5, 69.7, 65.8, 65.7, 56.4, 55.6, 52.9, 41.9, 33.7, 32.8, 32.0, 30.6, 28.9, 24.8. MALDI-TOFMS: $[\text{M} + \text{Na}^+]$ calcd for $\text{C}_{34}\text{H}_{53}\text{N}_9\text{O}_{19}\text{Na}^+$, 914.3350; found, 914.3320.

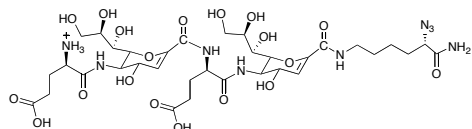
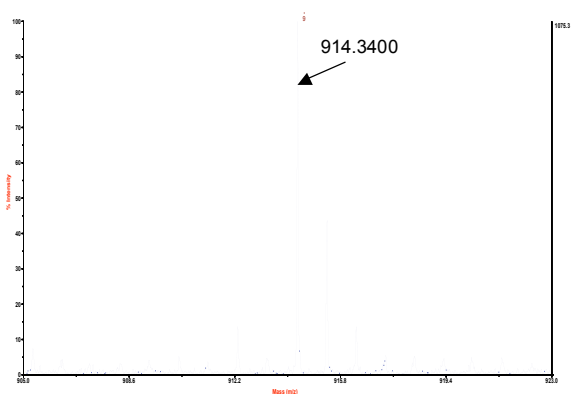


Neu2en/L-Glu-6 (10): obtained in 15% purified yield. ¹H NMR (D₂O, 600 MHz): δ 5.88 (d, 1H, *J* = 2.4 Hz, H3-2), 5.87 (d, 1H, *J* = 2.4 Hz, H3-4), 5.82 (d, 1H, *J* = 2.4 Hz, H3-6), 4.54 (dd, 3H, 9.0, 3.0 Hz, H4-2/4/6), 4.43-4.37 (m, 5H, H6-6, H α -5, H6-4, H α -3, H6-2), 4.22 (dd, 1H, *J* = 10.2, 8.4 Hz, H5-2), 4.17-4.11 (m, 3H, H α -7, H5-4/6), 4.08 (t, 1H, *J* = 6.6 Hz, H α -1), 4.01 (ddd, 1H, *J* = 9.0, 5.4, 2.4 Hz, H8-2), 3.97 (ddd, 1H, *J* = 12.0, 6.0, 2.4 Hz, H8-4), 3.92-3.86 (m, 3H, H8-C_a, H9²-2/4), 3.91-3.85 (m, 7H, H7-2/4/6, H9-2/4/6, H9²-6), 3.36-3.28 (m, 2H, H ϵ -7), 2.45-2.35 (m, 6H, H γ -1/3/5), 2.18-2.07 (m, 6H, H β -1/3/5), 1.78-1.88 (m, 2H, H β -7), 1.65-1.59 (m, 2H, H δ -7), 1.44 (p, 2H, *J* = 7.8 Hz, H γ -7). ¹³C NMR (D₂O, 150 MHz): δ 179.9, 179.8, 178.7, 177.9, 176.0, 172.4, 166.2, 166.1, 166.0, 148.1, 147.4, 111.7, 111.5, 111.0, 78.8, 72.7, 72.5, 70.5, 69.5, 66.5, 65.8, 65.6, 57.1, 56.0, 52.8, 52.7, 41.8, 35.6, 33.7, 30.7, 30.1, 24.8. MALDI-TOFMS: [M + Na⁺] calcd for C₄₈H₇₃N₁₁O₂₈Na⁺, 1274.4518; found, 1274.456.



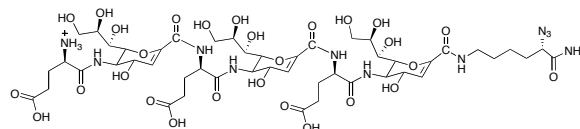
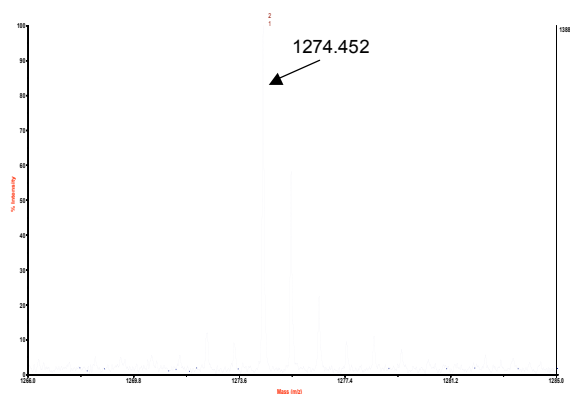
L-Glu/Neu2en-4 (11): obtained in 24% purified yield. ^1H NMR (D_2O , 600 MHz): d 5.96 (d, 1H, $J = 2.4$ Hz, H3-1), 5.91 (d, 1H, $J = 2.4$ Hz, H3-3), 4.67 (dd, 1H, $J = 8.4, 3.0$ Hz, H4-1), 4.64 (dd, 1H, $J = 9.6, 2.4$ Hz, H6-1), 4.57 (dd, 1H, $J = 9.0, 2.4$ Hz, H4-3), 4.52 (dd, 1H, $J = 8.4, 5.4$ Hz, $\text{H}\alpha$ -2), 4.44 (dd, 1H, $J = 7.2, 4.2$ Hz, $\text{H}\alpha$ -4), 4.44 (dd, 1H, $J = 10.8, 1.2$ Hz, H6-3), 4.19 (dd, 1H, $J = 10.8, 9.0$ Hz, H5-3), 4.15 (dd, 1H, $J = 7.2, 5.4$ Hz, $\text{H}\alpha$ -5), 4.08 (ddd, 1H, $J = 9.0, 6.0, 3.0$ Hz, H8-1), 4.00 (ddd, 1H, $J = 9.0, 6.0, 3.0$ Hz, H8-3), 3.94 (dd, 1H, $J = 12.0, 3.0$ Hz, H9'-1), 3.92 (dd, 1H, $J = 8.4, 1.2$ Hz, H7-1), 3.91 (dd, 1H, $J = 12.0, 3.0$ Hz, H9'-3), 3.80 (dd, 1H, $J = 12.0, 5.4$ Hz, H9-1), 3.72 (dd, 1H, $J = 9.6, 1.2$ Hz, H7-3), 3.71 (dd, 1H, $J = 12.0, 6.0$ Hz, H9-3), 3.66 (dd, 1H, $J = 9.6, 8.4$ Hz, H5-1), 3.31-3.22 (m, 2H, $\text{H}\epsilon$ -5), 2.57 (dd, 4H, $J = 7.2, 7.2$ Hz, $\text{H}\gamma$ '-2/4), 2.53 (dd, 4H, $J = 7.2, 7.2$ Hz, $\text{H}\gamma$ -2/4), 2.28-2.07 (m, 4H, $\text{H}\beta$ -2/4), 1.90-1.78 (m, 2H, $\text{H}\beta$ -5), 1.64-1.55 (m, 2H, $\text{H}\delta$ -5), 1.44 (p, 2H, $J = 7.8$ Hz, $\text{H}\gamma$ -5). ^{13}C NMR (D_2O , 150 MHz): d 180.3, 180.2, 178.4, 176.5, 175.6, 166.3, 165.9, 148.1, 148.0, 112, 110.9, 79.1, 77.9, 72.8, 72.7, 70.7, 70.5, 69.7, 67.6, 66.0, 65.8, 65.4, 56.4, 56.3, 53.7, 52.8, 41.9, 33.7, 33.0, 30.6, 29.2, 29.0, 24.8. MALDI-TOFMS: $[\text{M} + \text{Na}^+]$ calcd for $\text{C}_{34}\text{H}_{53}\text{N}_9\text{O}_{19}\text{Na}^+$, 914.3350; found, 914.3330.

Figure S1. Mass spectra of α/δ -hybrid peptides (**5-12**).



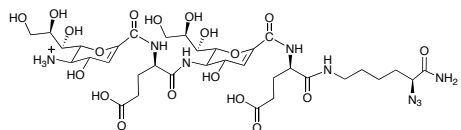
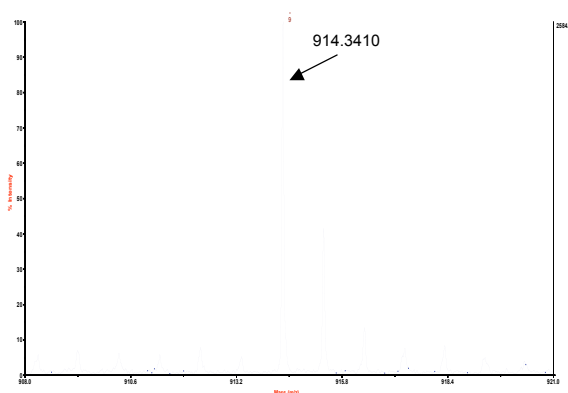
5

$C_{34}H_{53}N_9O_{19}Na^+$
 Found = 914.3400
 Theor. = 914.3350



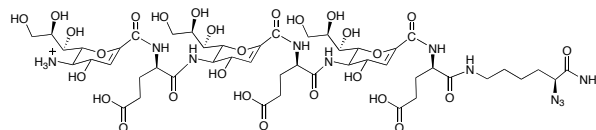
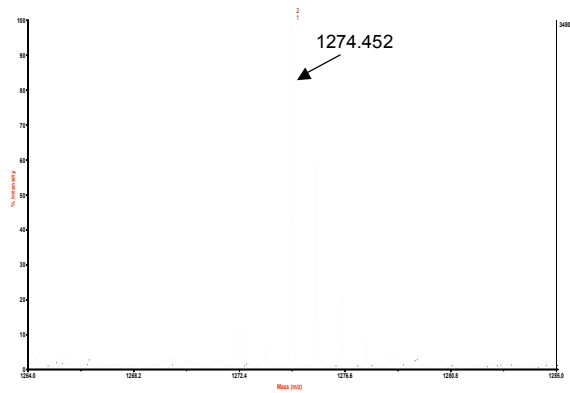
6

$C_{48}H_{73}N_{11}O_{28}Na^+$
 Found = 1274.452
 Theor. = 1274.4518



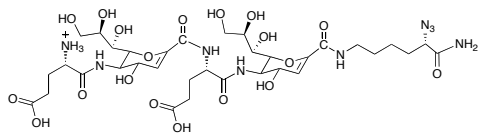
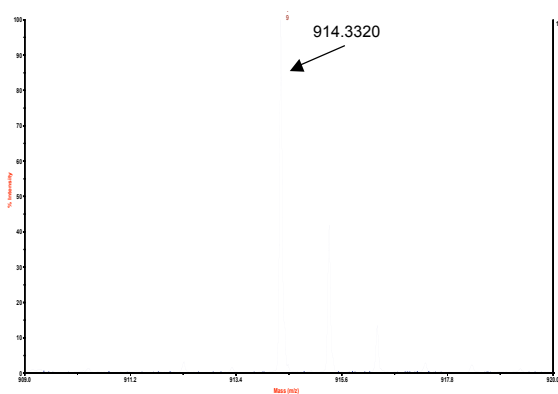
7

$C_{34}H_{53}N_9O_{19}Na^+$
 Found = 914.3410
 Theor. = 914.3350



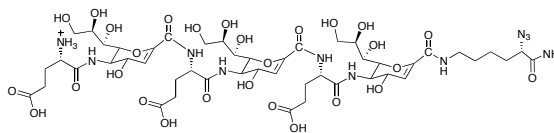
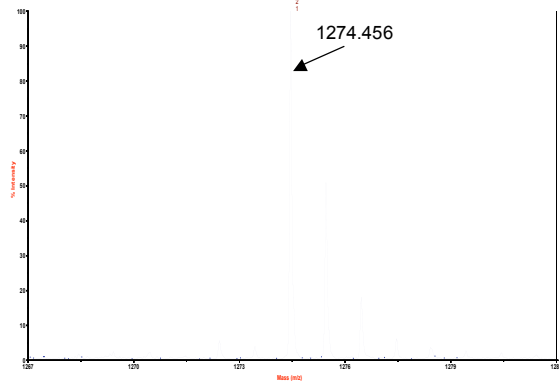
8

$C_{48}H_{73}N_{11}O_{28}Na^+$
 Found = 1274.452
 Theor. = 1274.4518



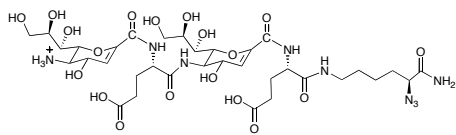
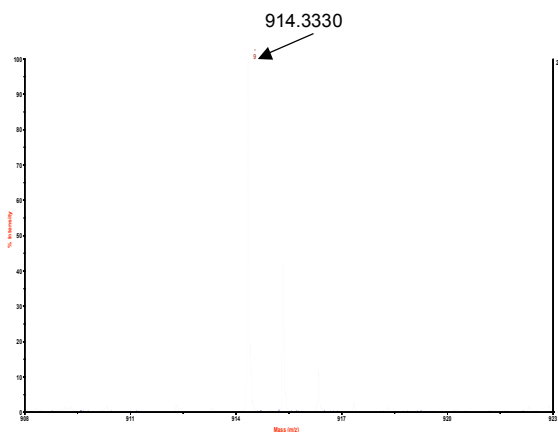
9

$C_{34}H_{53}N_9O_{19}Na^+$
 Found = 914.3320
 Theor. = 914.3350



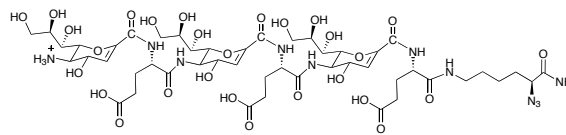
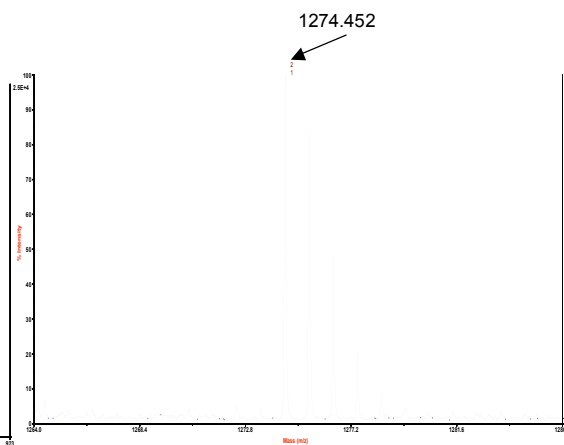
10

$C_{48}H_{73}N_{11}O_{28}Na^+$
 Found = 1274.456
 Theor. = 1274.4518



11

$C_{34}H_{53}N_9O_{19}Na^+$
 Found = 914.3330
 Theor. = 914.3350



12

$C_{48}H_{73}N_{11}O_{28}Na^+$
 Found = 1274.452
 Theor. = 1274.4518

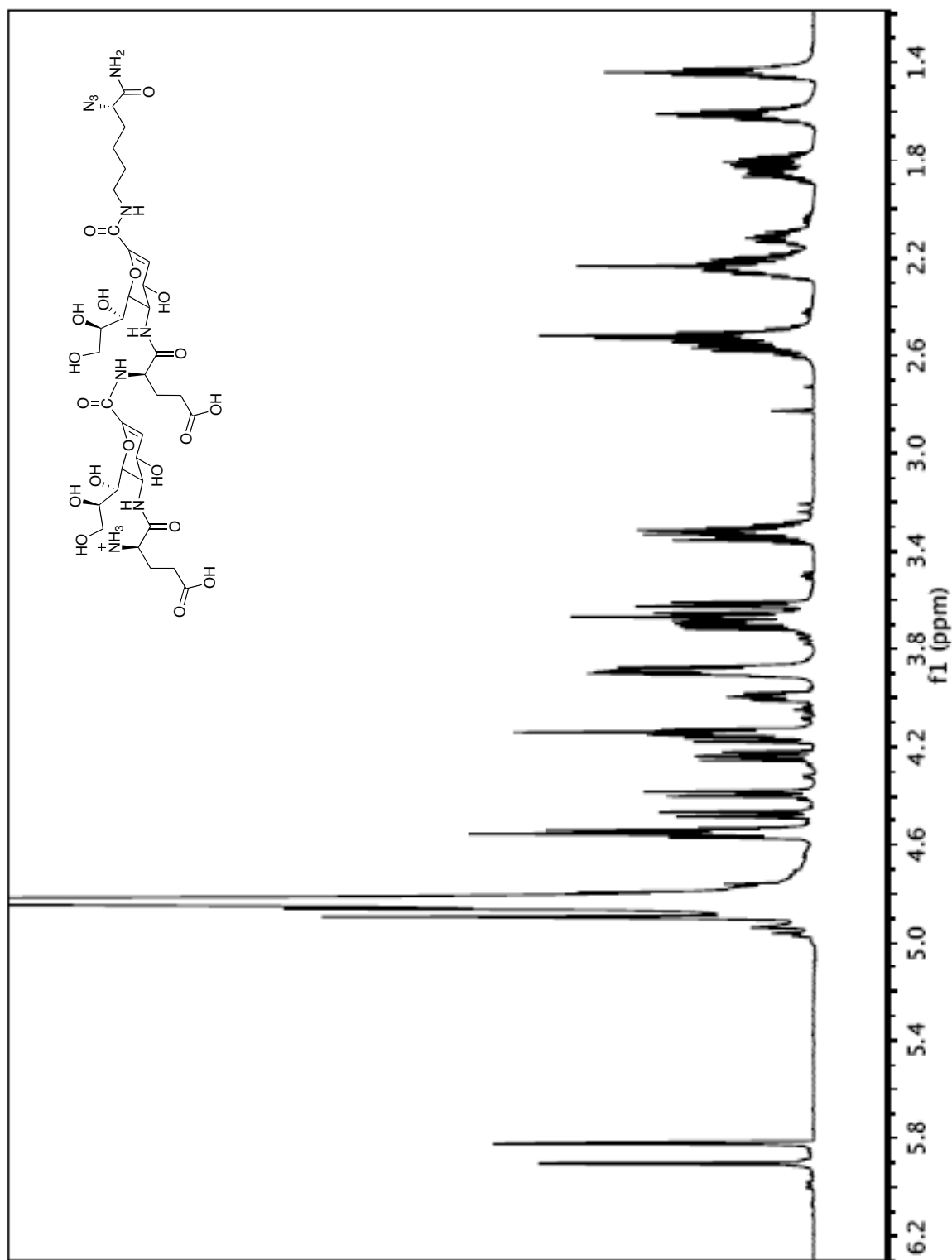


Figure S2. ¹H NMR spectrum of α/δ-hybrid peptide 5.

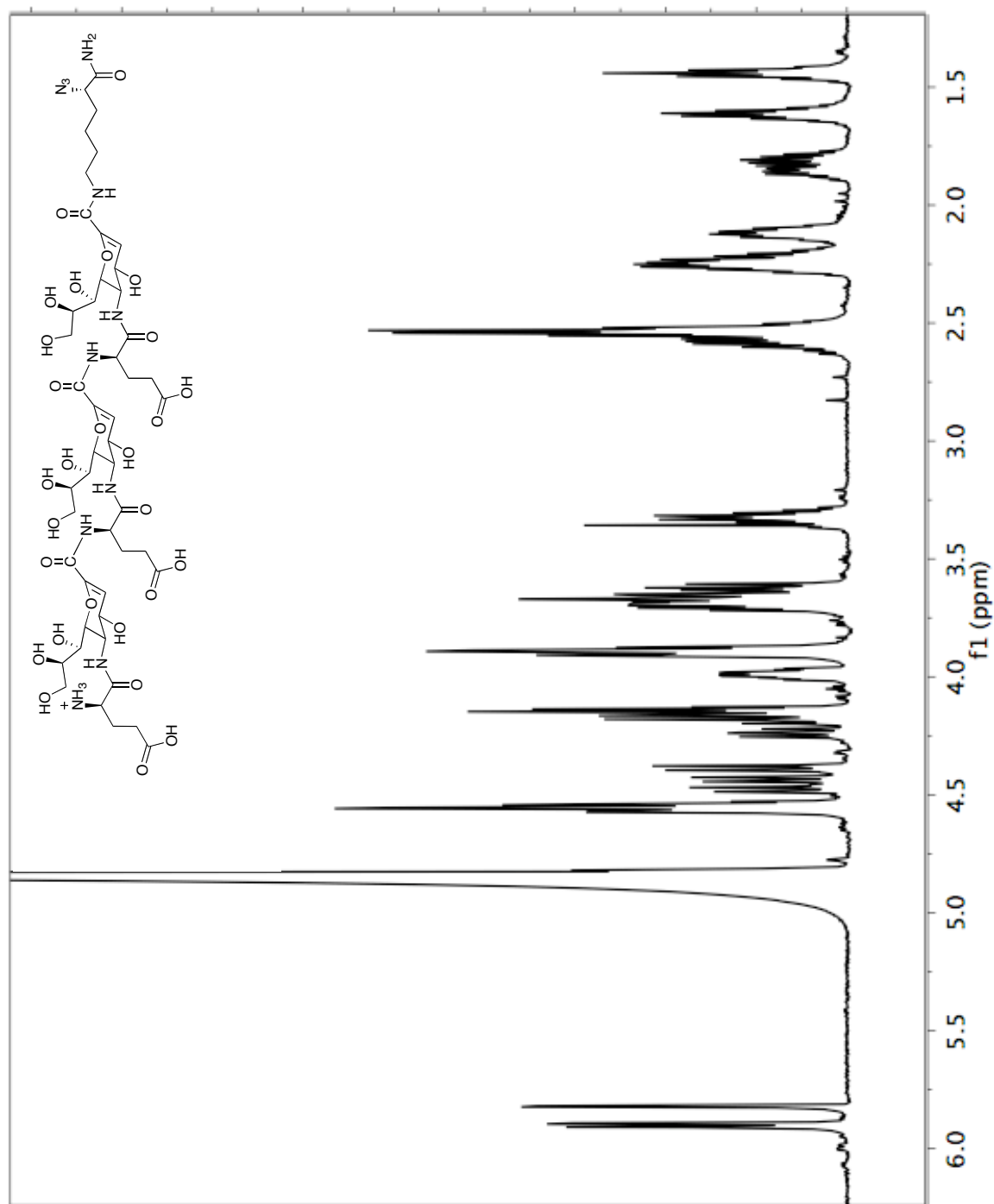


Figure S3. ^1H NMR spectrum of α/δ -hybrid peptide **6**.

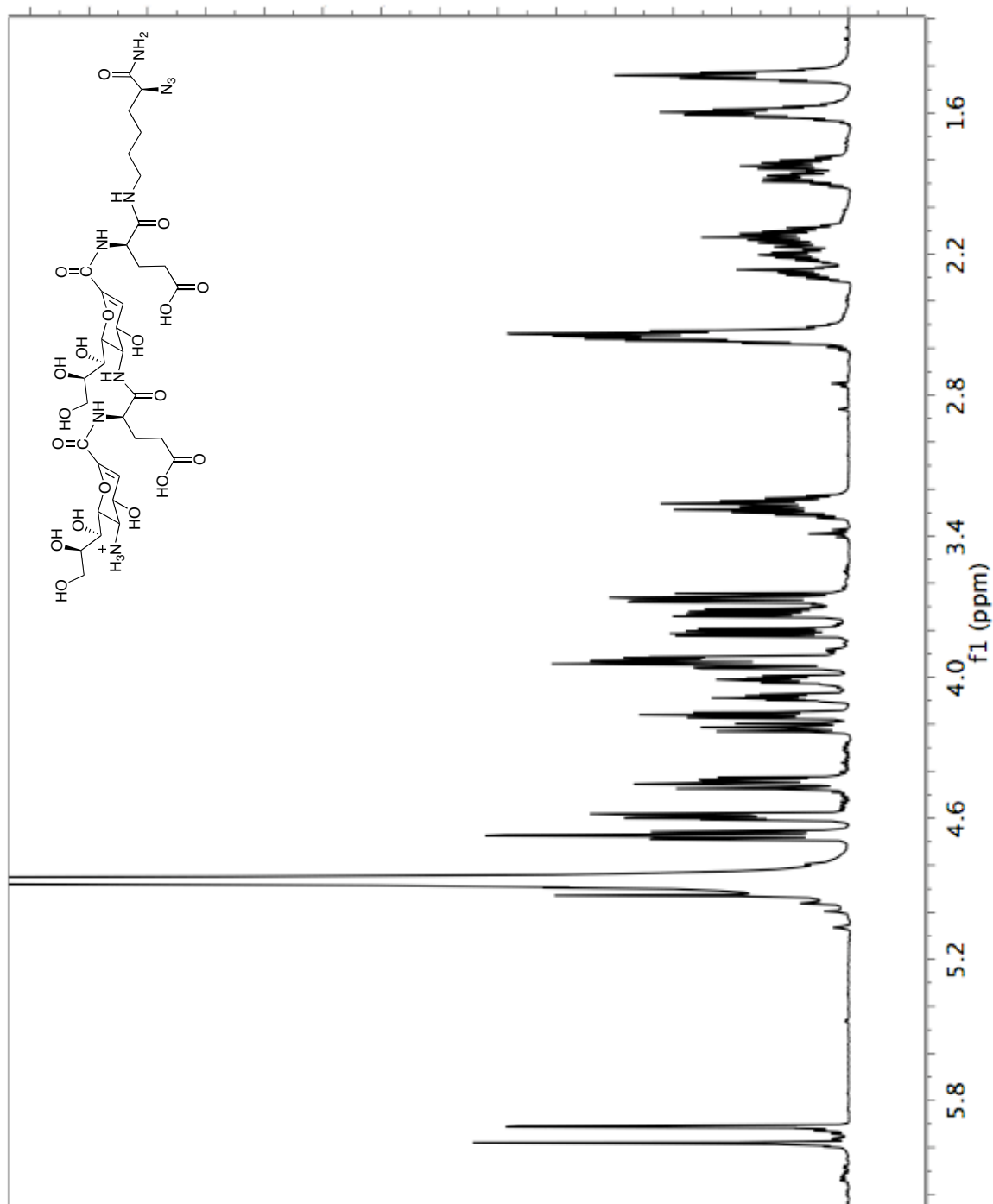


Figure S4. ^1H NMR spectrum of α/δ -hybrid peptide 7.

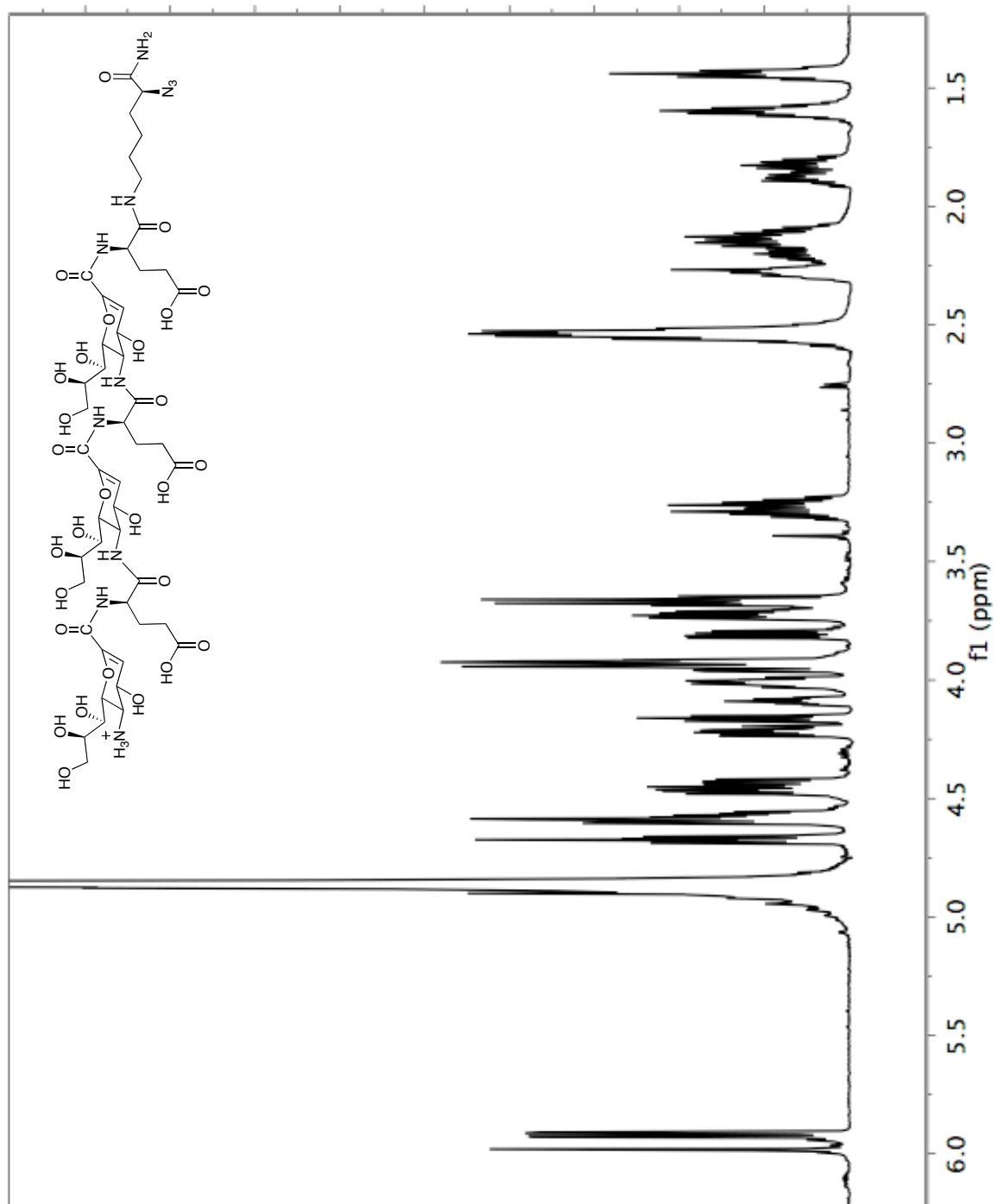


Figure S5. ¹H NMR spectrum of α/δ-hybrid peptide **8**.

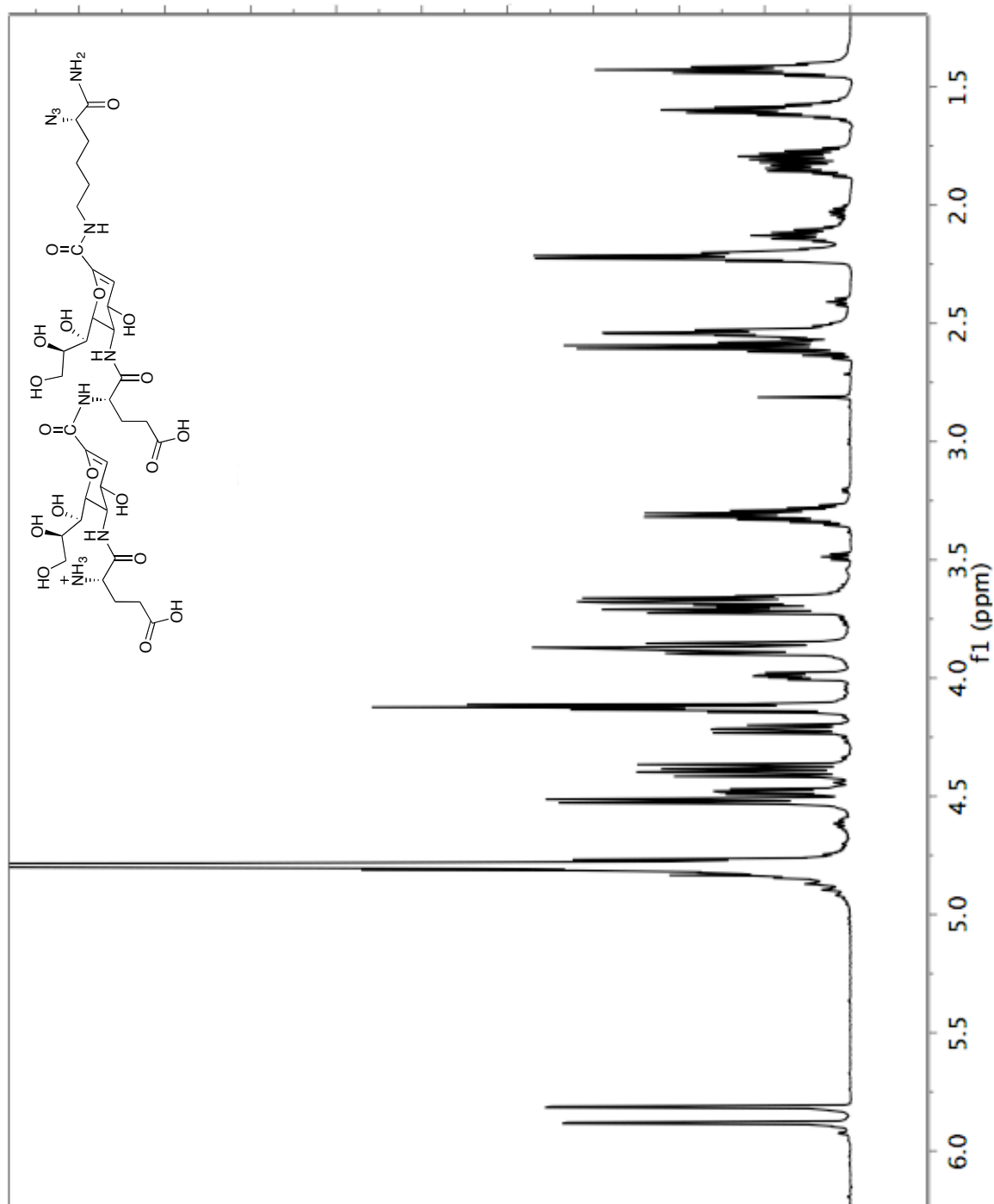


Figure S6. ^1H NMR spectrum of α/δ -hybrid peptide **9**.

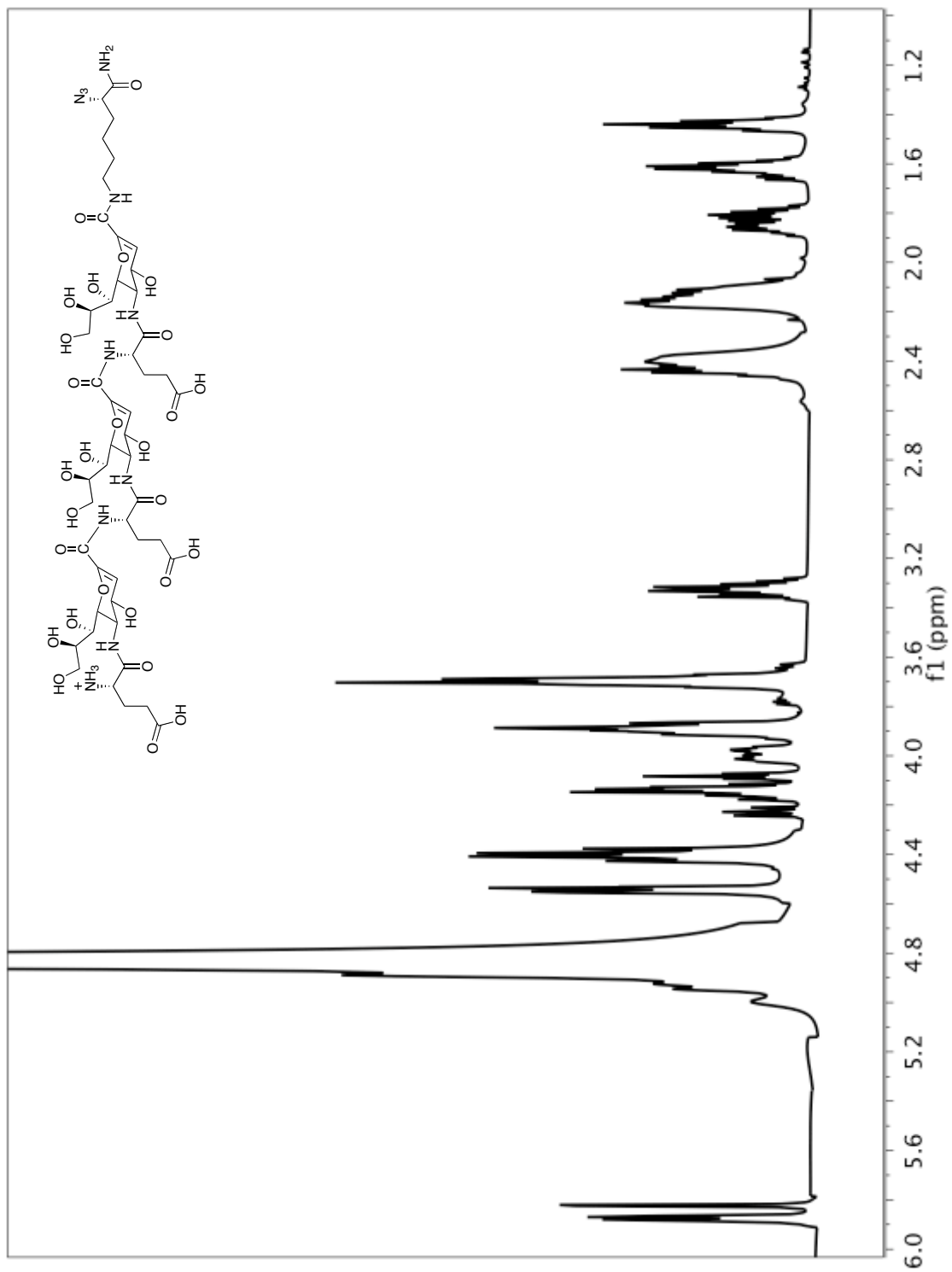


Figure S7. ¹H NMR spectrum of α/δ-hybrid peptide **10**.

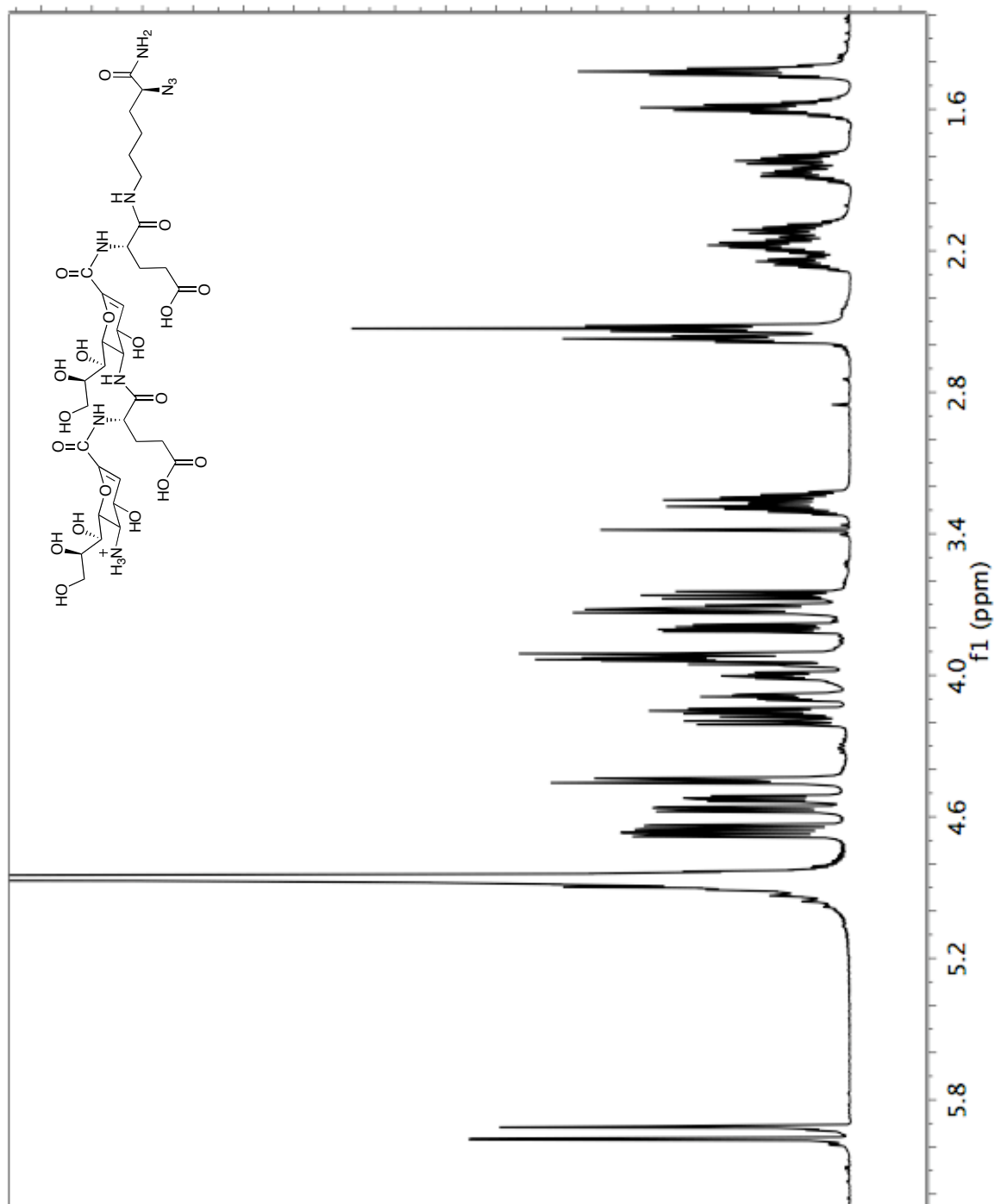


Figure S8. ^1H NMR spectrum of α/δ -hybrid peptide 11.

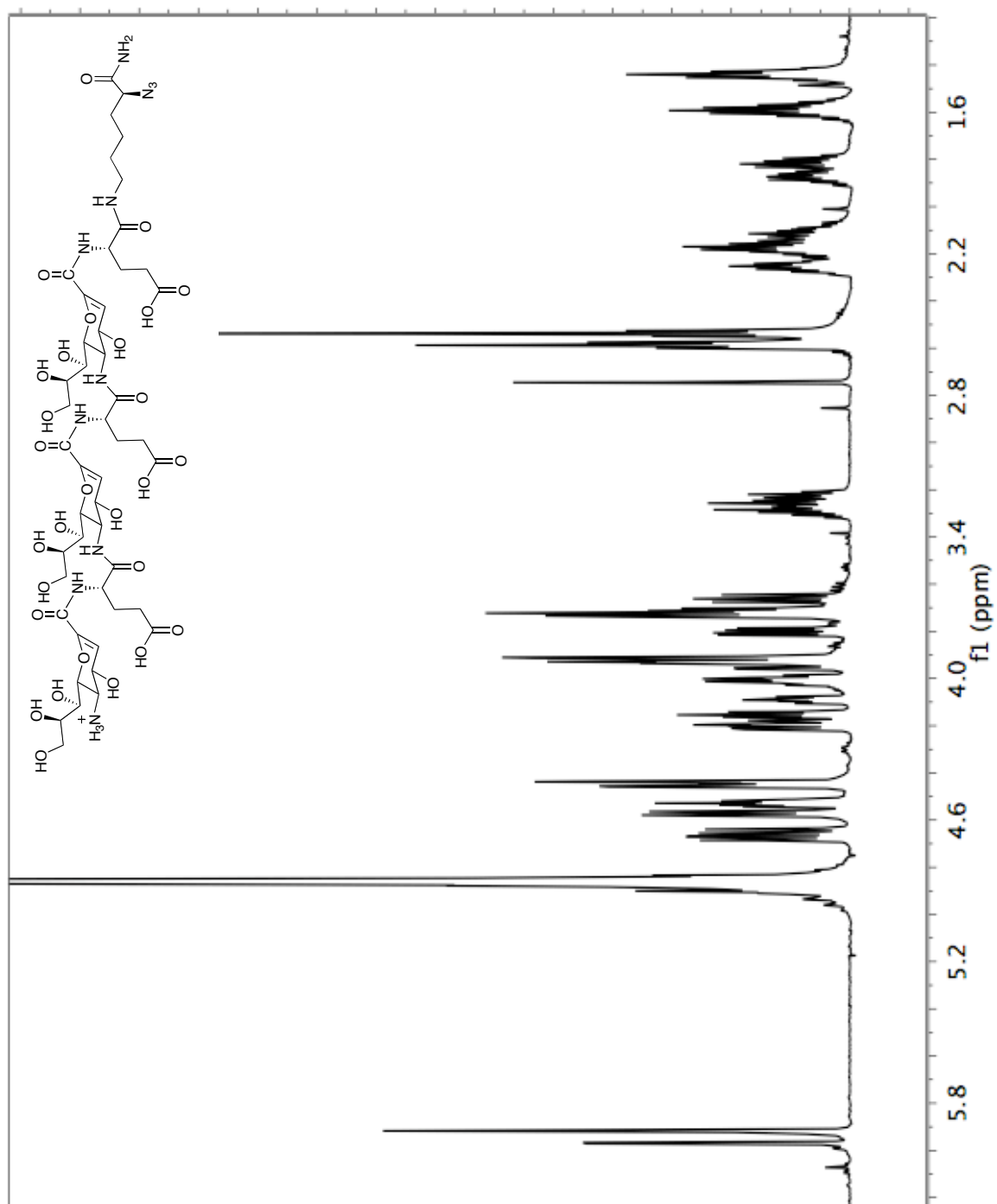


Figure S9. ^1H NMR spectrum of α/δ -hybrid peptide 12.

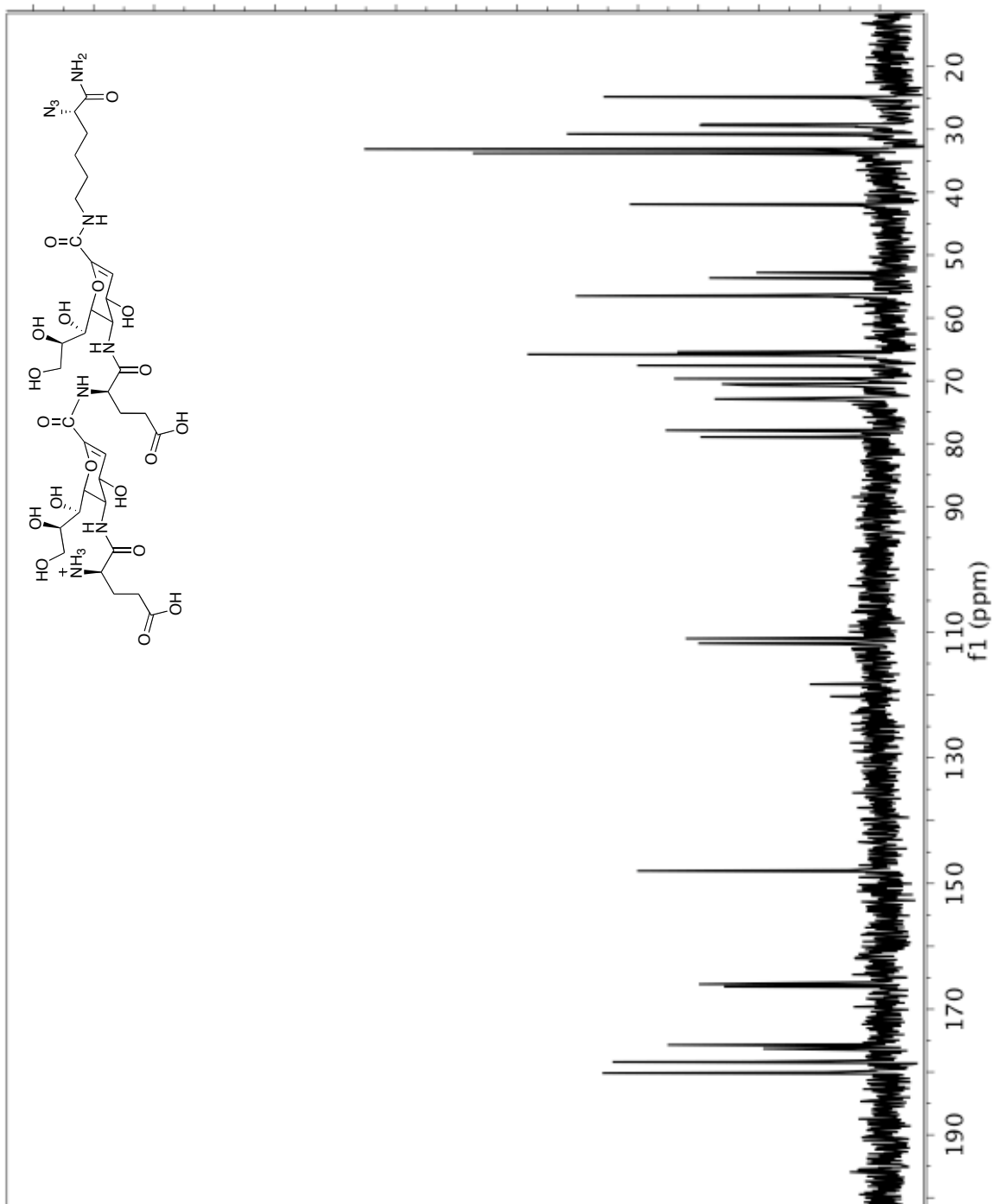


Figure S10. ^{13}C NMR spectrum of α/δ -hybrid peptide 5.

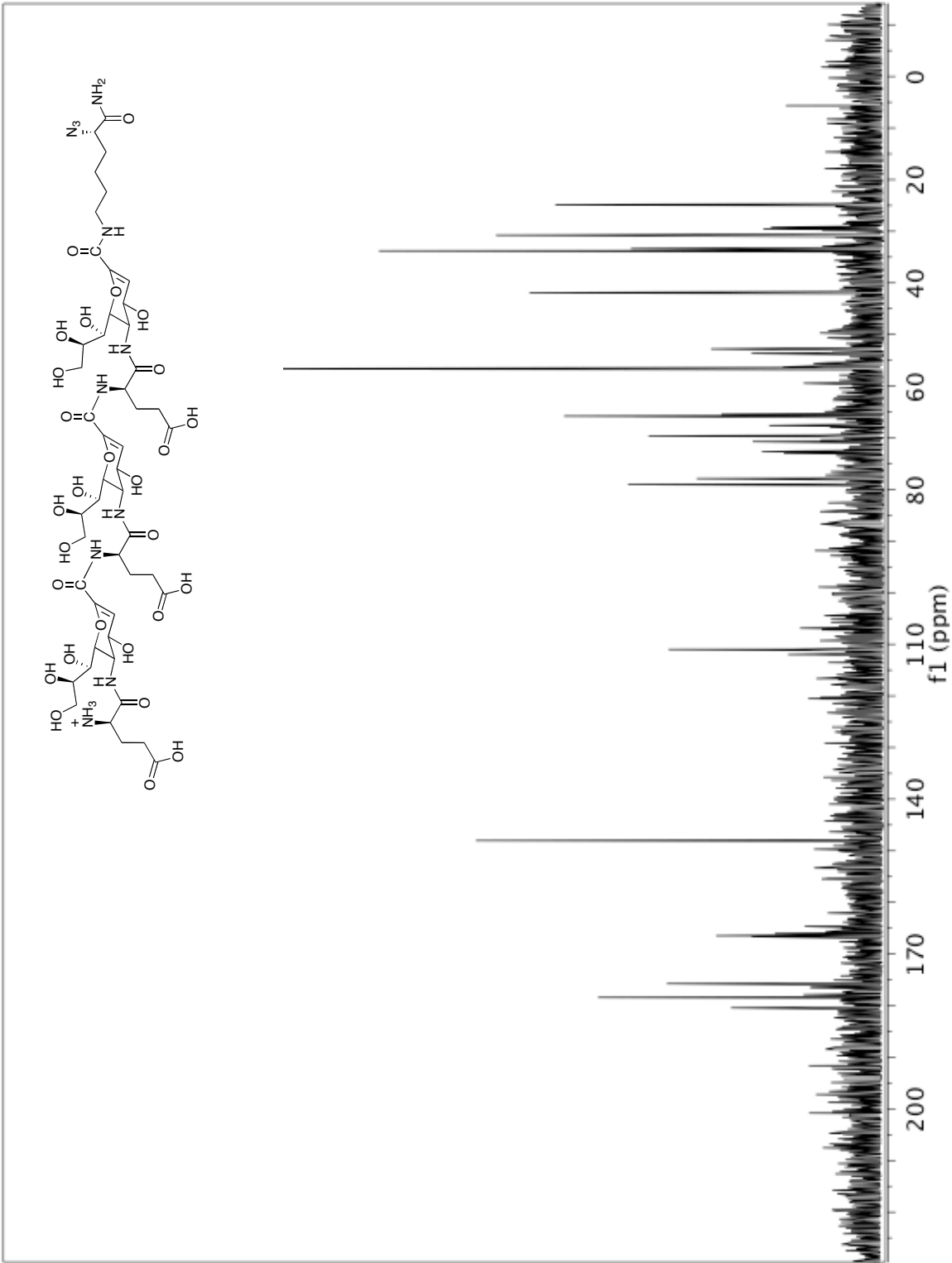


Figure S11. ^{13}C NMR spectrum of α/δ -hybrid peptide **6**.

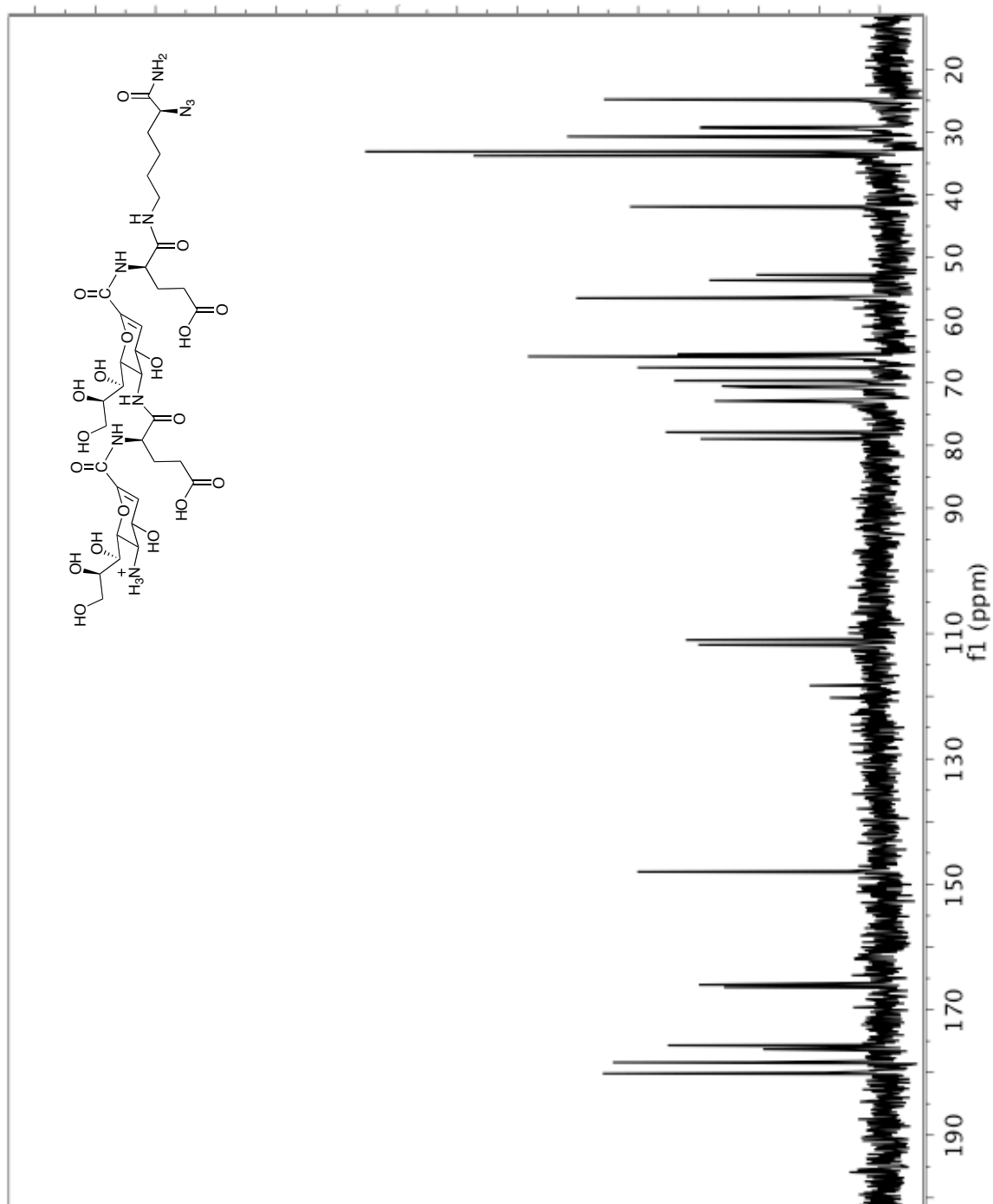


Figure S12. ^{13}C NMR spectrum of α/δ -hybrid peptide 7.

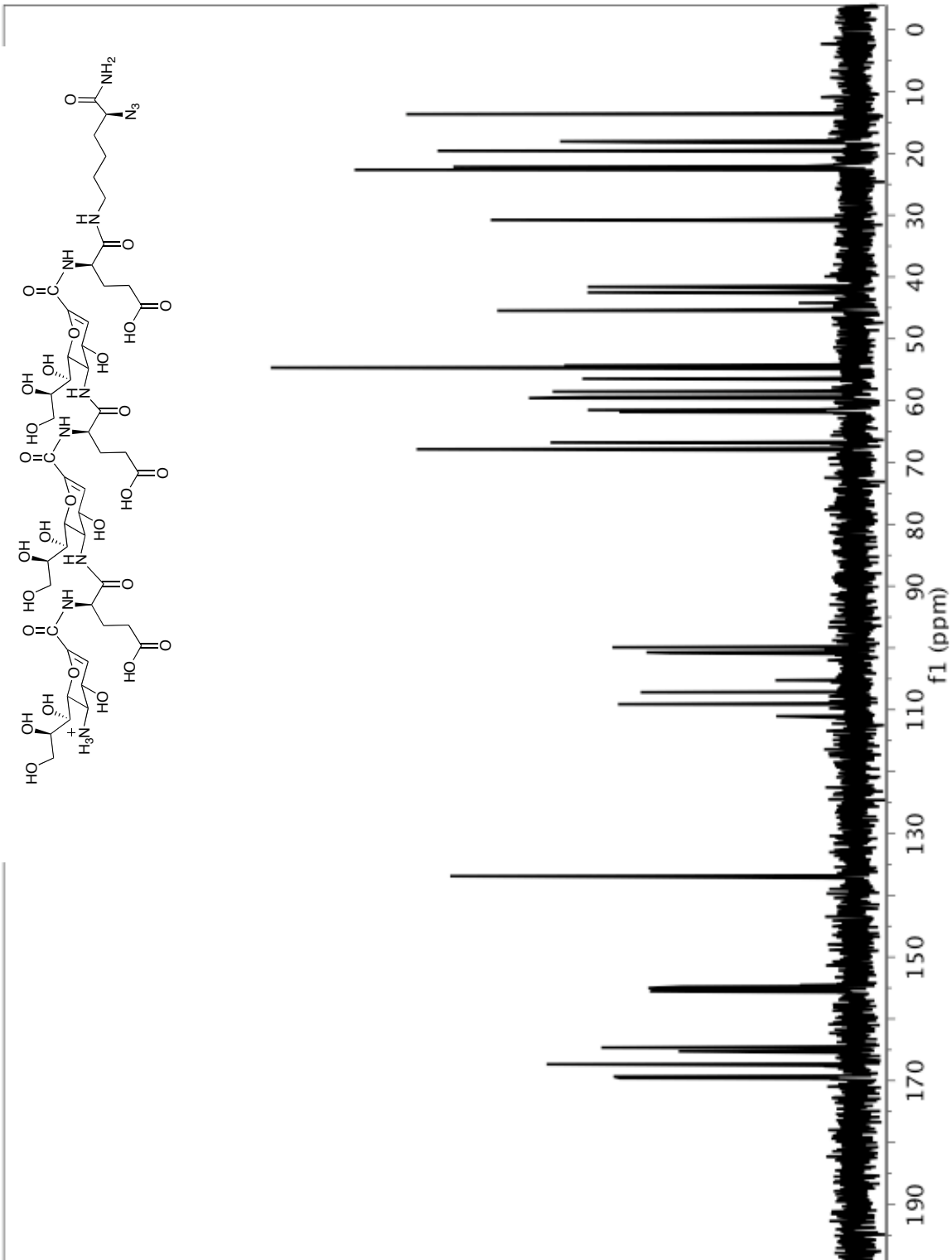


Figure S13. ^{13}C NMR spectrum of α/δ -hybrid peptide 8.

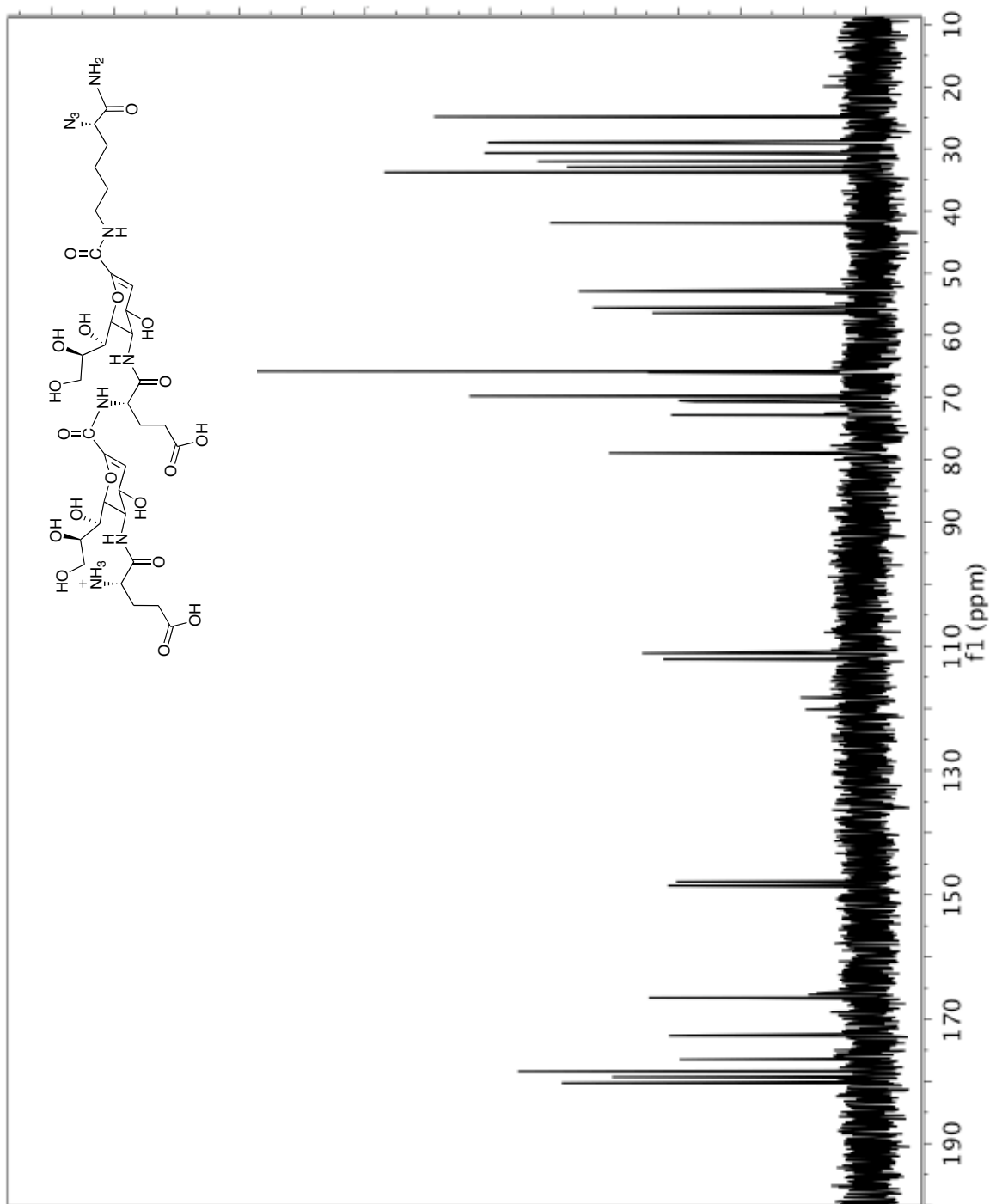


Figure S14. ^{13}C NMR spectrum of α/δ -hybrid peptide 9.

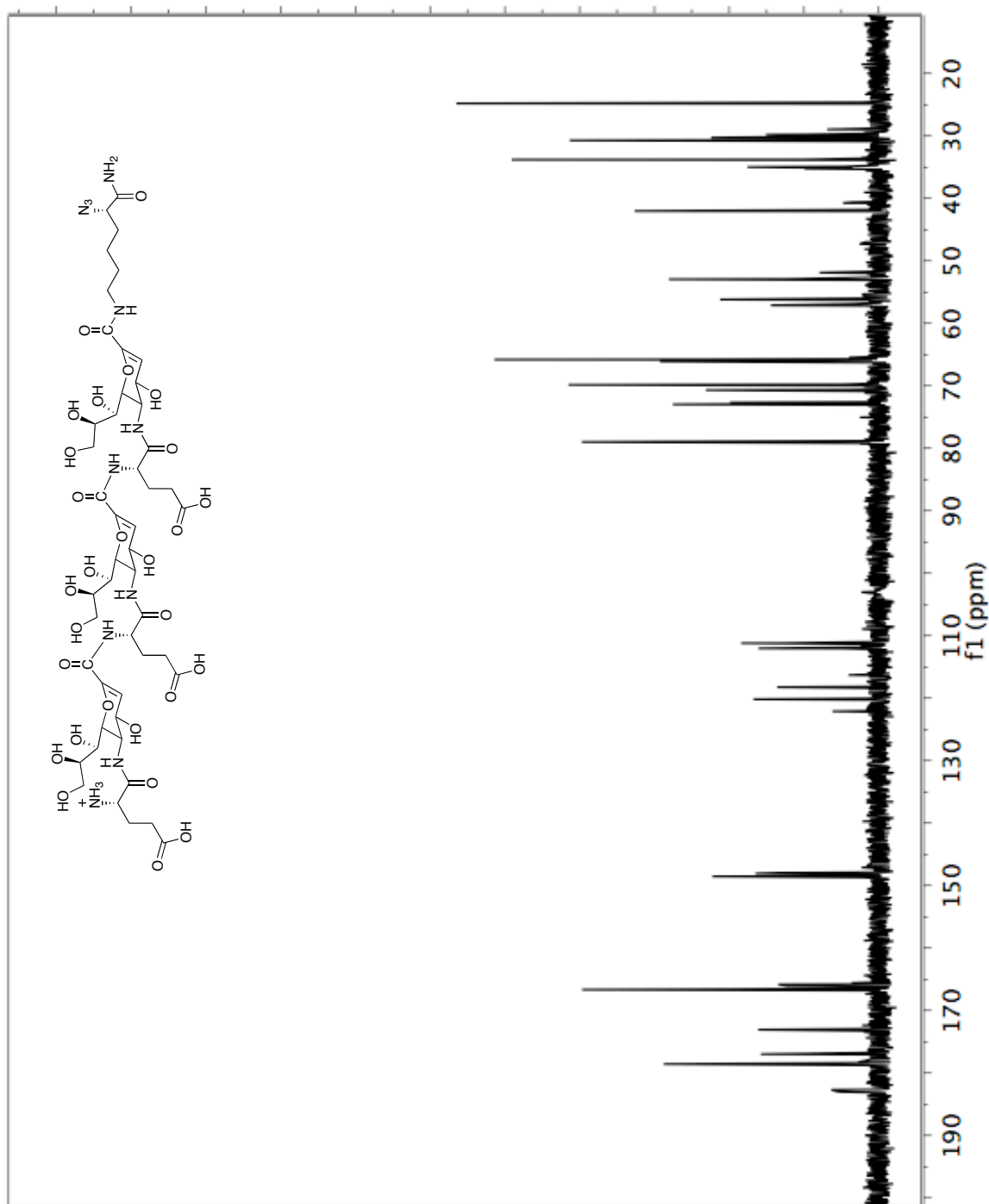


Figure S15. ^{13}C NMR spectrum of α/δ -hybrid peptide 10.

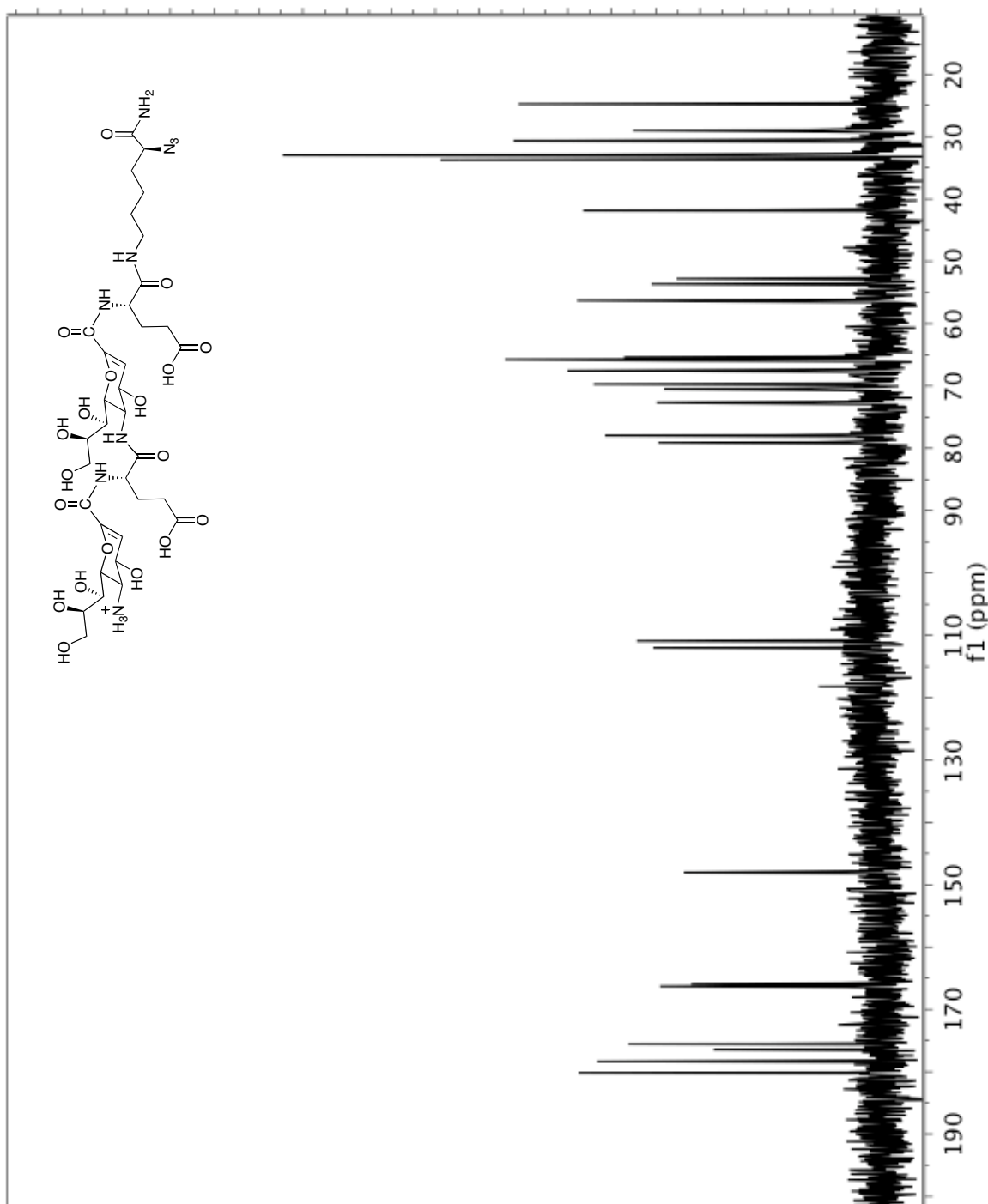


Figure S16. ^{13}C NMR spectrum of α/δ -hybrid peptide **11**.

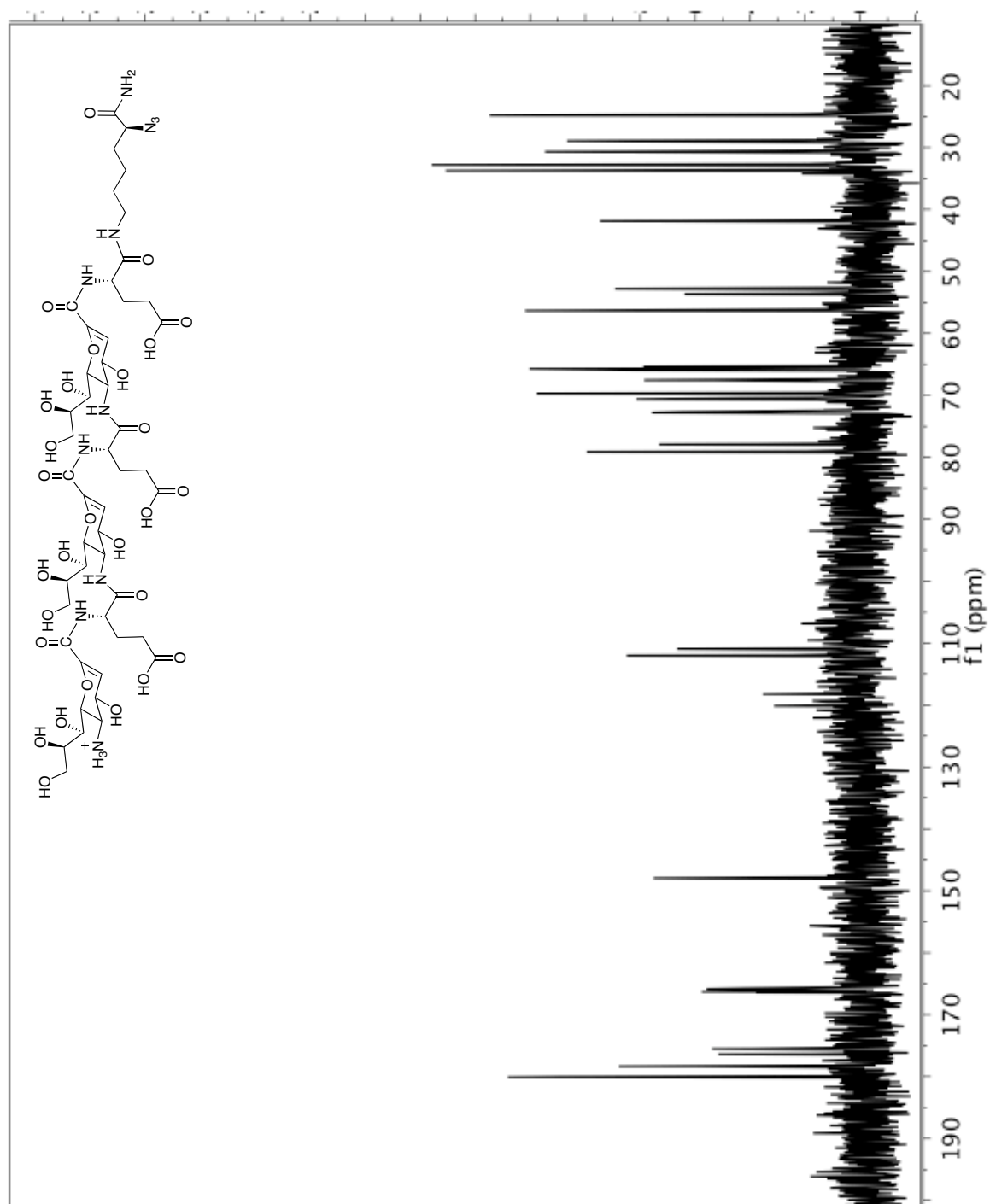


Figure S17. ^{13}C NMR spectrum of α/δ -hybrid peptide 12.

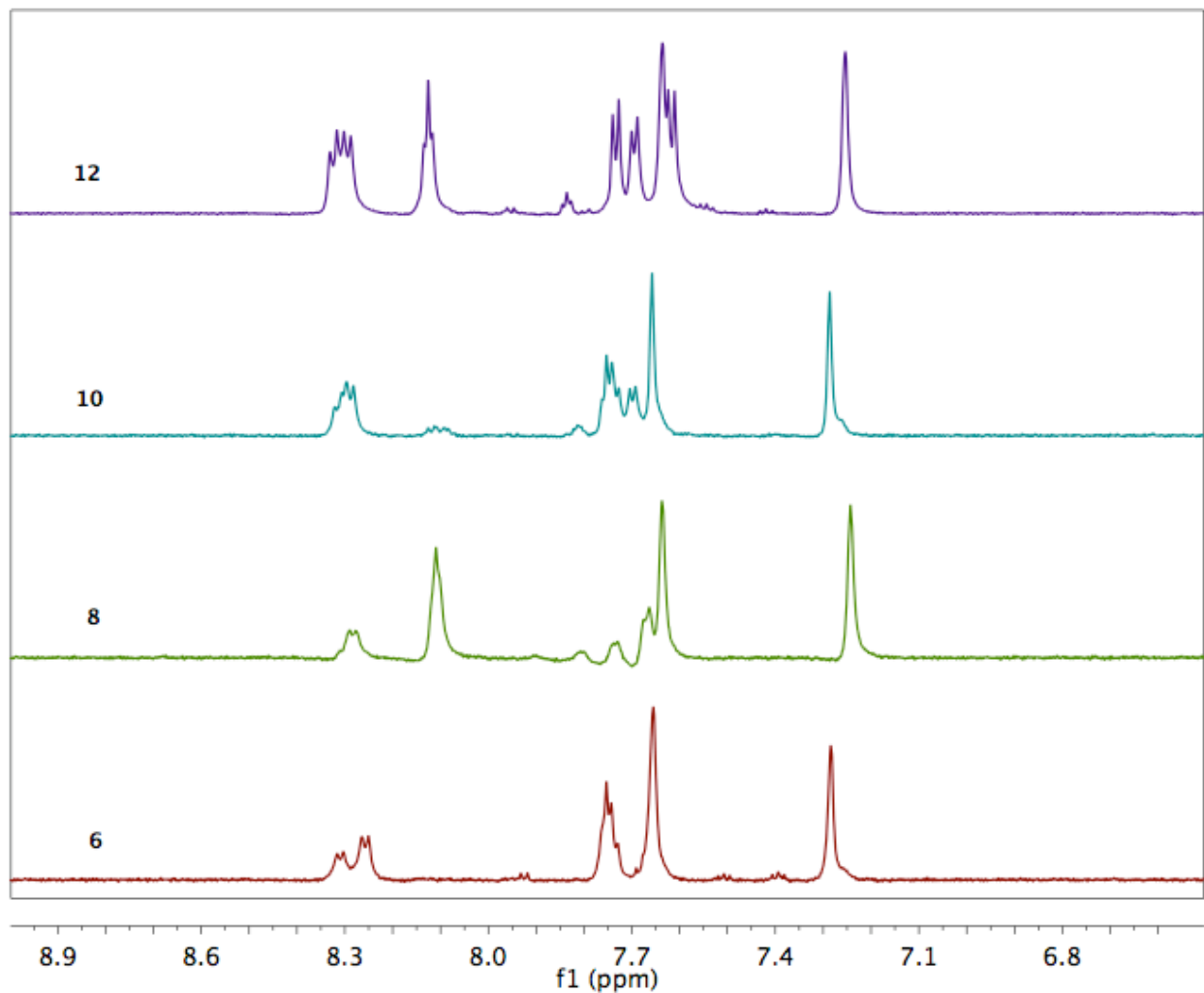


Figure S18. Stack plot of the amide regions from ¹H NMR spectra (DMSO-*d*₆ at 298 K, 600 MHz) showing that the amide H of **12** are more dispersed and distinct from each other compared to **6**, **8**, and **10**.

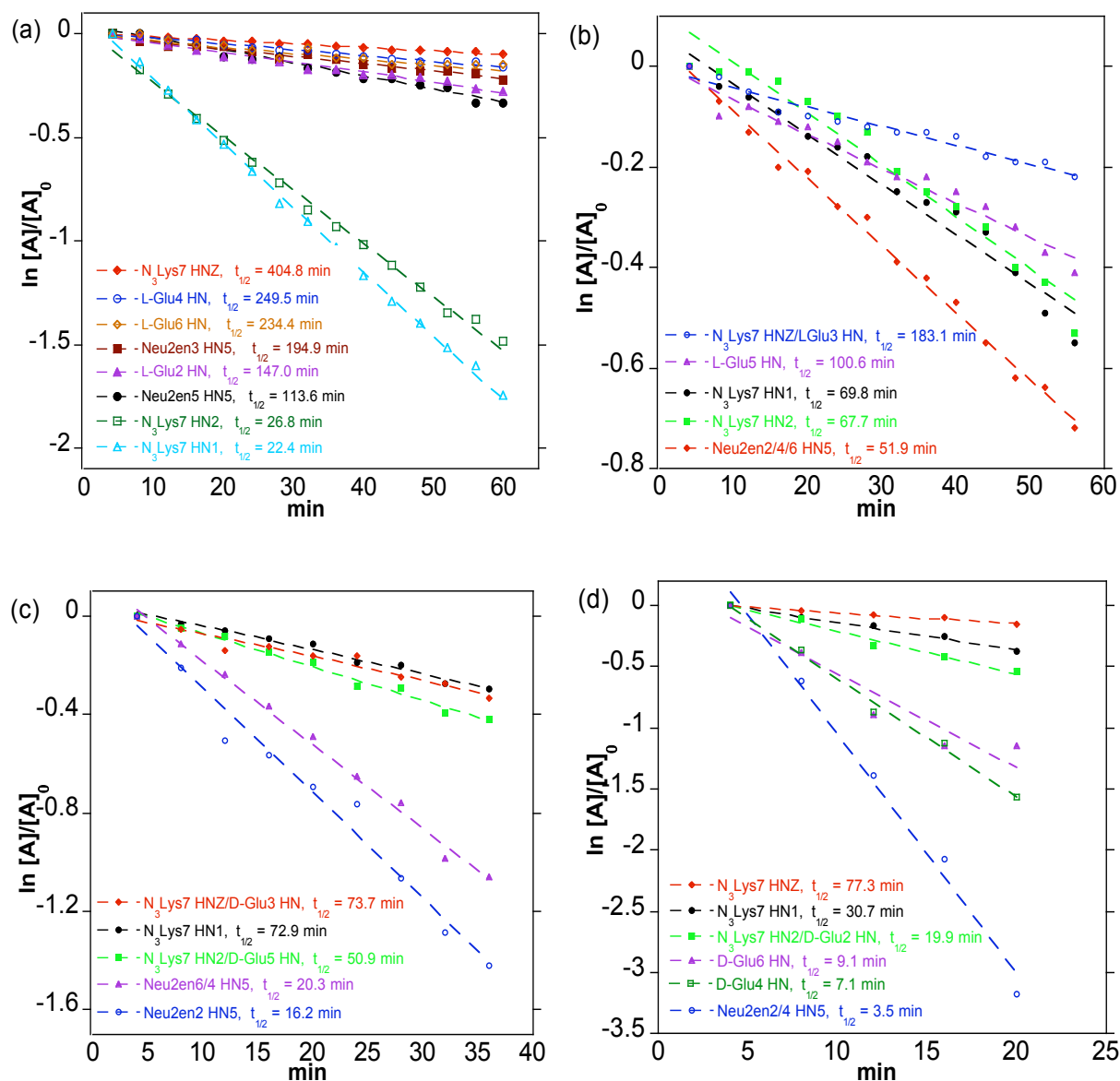


Figure S19. NH/ND exchange study for **6**, **8**, **10**, and **12** in DMSO- d_6 at 298 K, 600 MHz. Pseudo first order rate plots showing the long $t_{1/2}$ of H-bonded amide protons of **12** (a) indicating a 2° structure stabilized by intramolecular amide H-bonds. The amide H of **6** (c) and **8** (d) have relatively shorter $t_{1/2}$ of 3-20 min indicating unfolded peptide chain while those of **10** (b) have $t_{1/2}$ of 52-100 min that are equivalent to about double the NH/ND exchange rate of **12**.

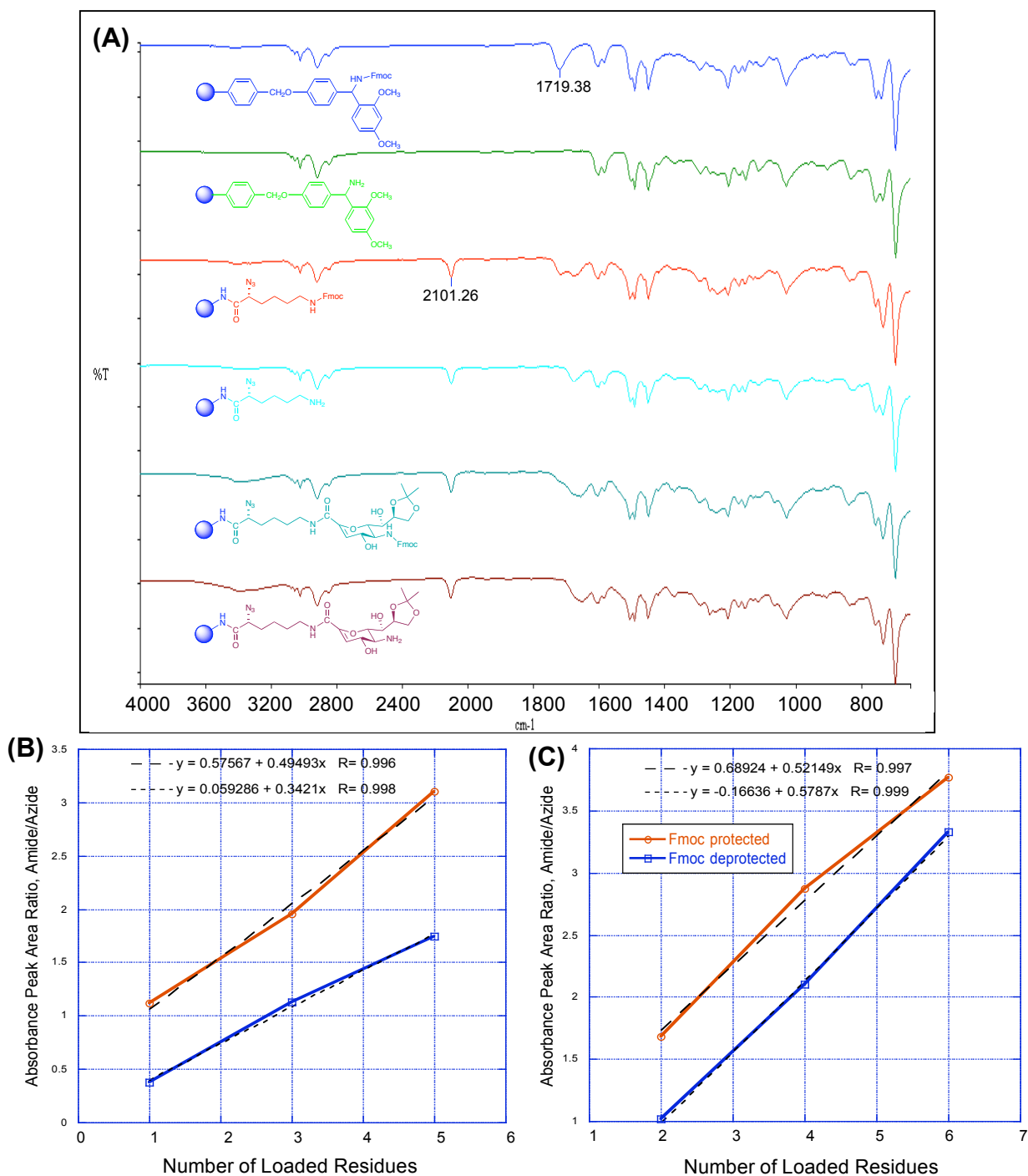
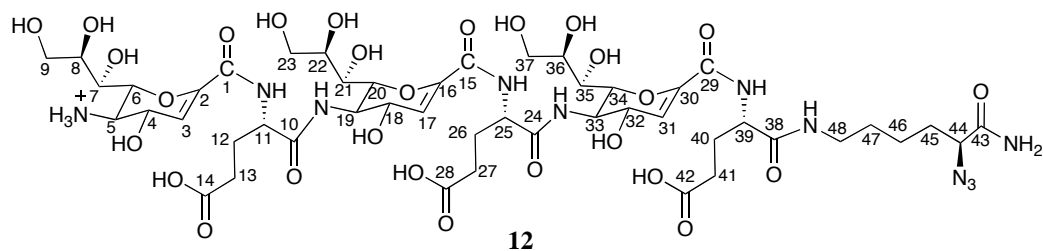
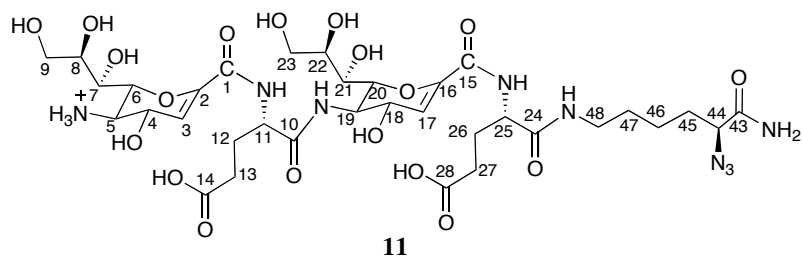


Figure S20. (A) Stack plot of IR spectra for on-bead monitoring of SPPS using the synthesis of **8** as an example. Absorption bands at 1719 cm^{-1} due to C=O of Fmoc, 2101 cm^{-1} due to N_3 . (B) and (C) Plots of amide/azide IR band peak area integration showing the linear correlation as a function of peptide length: (B) Odd numbered* residues, (C) even numbered* residues. red plot: oligomer with Fmoc protected *N*-terminus; blue plot: oligomer with deprotected *N*-terminus. **N.B.* Number system is based on the growing peptide chain bound to N_3Lys on the bead, *i.e.* Glu6 is loaded residue number 1.

Assignment strategy for the NMR chemical shifts of 11 and 12. NMR characterization of **12** proved to be challenging because of very close and overlapping peaks in its ^1H NMR spectra. Our previous report on amide-linked Neu2en polymers¹ made it possible to distinguish between the downfield H3 proton of *N*-terminal from internal Neu2en residue. This distinction proved to be crucial in our strategy for **12**. We began the characterization with H ϵ (δ 3.22-3.31) of N₃Lys-7 of **11** because it is an unambiguous aminomethylene, and walked through the residue to completely assign the protons using homonuclear COSY. Next, we used Neu2en H3 as a reporter atom that distinguished Neu2en-1 (δ 5.96) from Neu2en-3 (δ 5.91). Assignment of proton resonances was accomplished by separately walking through intraresidue connectivities of terminal and internal Neu2en residues using homonuclear COSY, while one-bond C \rightarrow H connectivities were accomplished using HSQC. Another approach was used to connect the amino acid residues and differentiate the two L-Glu residues since their H α 's have different chemical shifts: L-Glu-2 (H α , δ 4.52) and L-Glu-4 (H α , δ 4.44). L-Glu-4 H α was assigned using HMBC since we found strong correlations that allowed us to unambiguously identify L-Glu-4: L-Glu-4 C=O \rightarrow H α of L-Glu-4 and L-Glu-4 C=O \rightarrow H ϵ of N₃Lys. By deduction, we assigned the other H α to L-Glu-2. Following the same approach that we used for **11**, we assigned the proton resonances of **12** using Neu2en H3 as reporter atom. Neu2en-1 has a unique set of ^1H NMR resonance peaks. Overlapping peaks were found for H4, H6, H7, H9, and H9' of Neu2en-3 and -5 and these resonances were assigned to both, while their H5 and H8 were very distinct. Neu2en-5 and L-Glu-6 were identified using the following HMBC correlations: L-Glu-6 C=O \rightarrow H ϵ of N₃Lys, L-Glu-6 C=O \rightarrow H α of L-Glu-6 and Neu2en-5 C=O \rightarrow H α of L-Glu-6. We also found another HMBC correlations for the following: Neu2en-3 C=O \rightarrow H α of L-Glu-4 and Neu2en-1 C=O \rightarrow H α of L-Glu-2. Furthermore, H β and H γ of all L-Glu residues are overlapped for both **11** and **12** and we were not able to differentiate them, so all L-Glu H β and H γ were assigned the same chemical shifts. The table for **11** and **12** below summarizes our approach, which is the same strategy that we applied for **7**, **8**, **9**, and **10**.



#	11, H-H COSY ^a	11, HMBC ^{a,b}	12, H-H COSY ^a	12, HMBC ^{a,b}
Neu2en-1				
1	-	3	-	3, 11
2	-	3	-	3, 4
3	4	4	4	4
4	3, 5	5, 6	3, 5	5, 6
5	4, 6	3, 4	4, 6	4, 6
6	5, 7	5, 7	5, 7	5, 7
7	6, 8	-	6, 8	-
8	7, 9, 9'	7	7, 9, 9'	-
9	8, 9'	-	8, 9'	-
9'	8, 9	-	8, 9	-
L-Glu-2				
10	-	11, 19	-	11, 12
11	12	12, 13	12	12, 13
12	11, 13	11, 13	11, 13	11, 13
13	12	11, 12	12	11, 12
14	-	13	-	13
Neu2en-3				
15	-	17	-	17, 25
16	-	17	-	17, 18
17	18	18	18	18
18	17, 19	19	17, 19	19, 20
19	18, 20	17, 18, 20	18, 20	17, 18, 20
20	19, 21	19	19, 21	19
21	20, 22	-	20, 22	19, 20
22	21, 23, 23'	21, 23	21, 23, 23'	21, 23, 23'
23	22, 23'	-	22, 23'	21
23'	22, 23	-	22, 23	-

L-Glu-4	24	-	25, 48	-	25, 26
	25	26	26, 27	26	26, 27
	26	25, 27	25, 27	25, 27	25, 27
	27	26	25, 26	26	25, 26
	28	-	27	-	26, 27
Neu2en-5	29	-	-	-	31, 39
	30	-	-	-	31
	31	-	-	32	32
	32	-	-	31, 33	33, 34
	33	-	-	32, 34	31, 32, 34
	34	-	-	33, 35	33
	35	-	-	34, 36	33, 34
	36	-	-	35, 37, 37'	35, 37
	37	-	-	36, 37'	35
	37'	-	-	36, 37	
L-Glu-6	38	-	-	-	39, 40, 48
	39	-	-	40	40, 41
	40	-	-	39, 41	39, 41
	41	-	-	40	39,40
	42	-	-	-	40, 41
N ₃ Lys-5 (7)	43	-	44	-	44, 45
	44	45	45, 46	45	45, 46
	45	44, 46	44, 46	44, 46	44, 46
	46	45, 47	44, 45, 48	45, 47	45, 47
	47	46, 48	45, 46, 48	46, 48	45, 46, 48
	48	47	46, 47	47	46, 47

^aD₂O, 600 MHz

^bHMBC correlations are from carbon atom #(s) in column 1 to the indicated proton; *J*_{C,H} at 8 Hz.

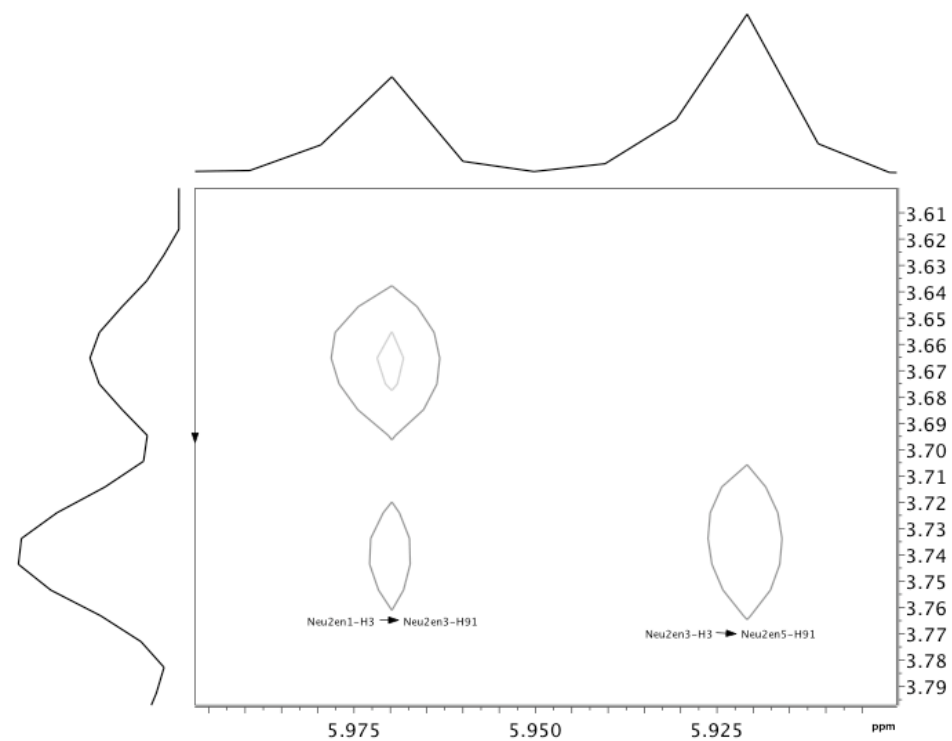
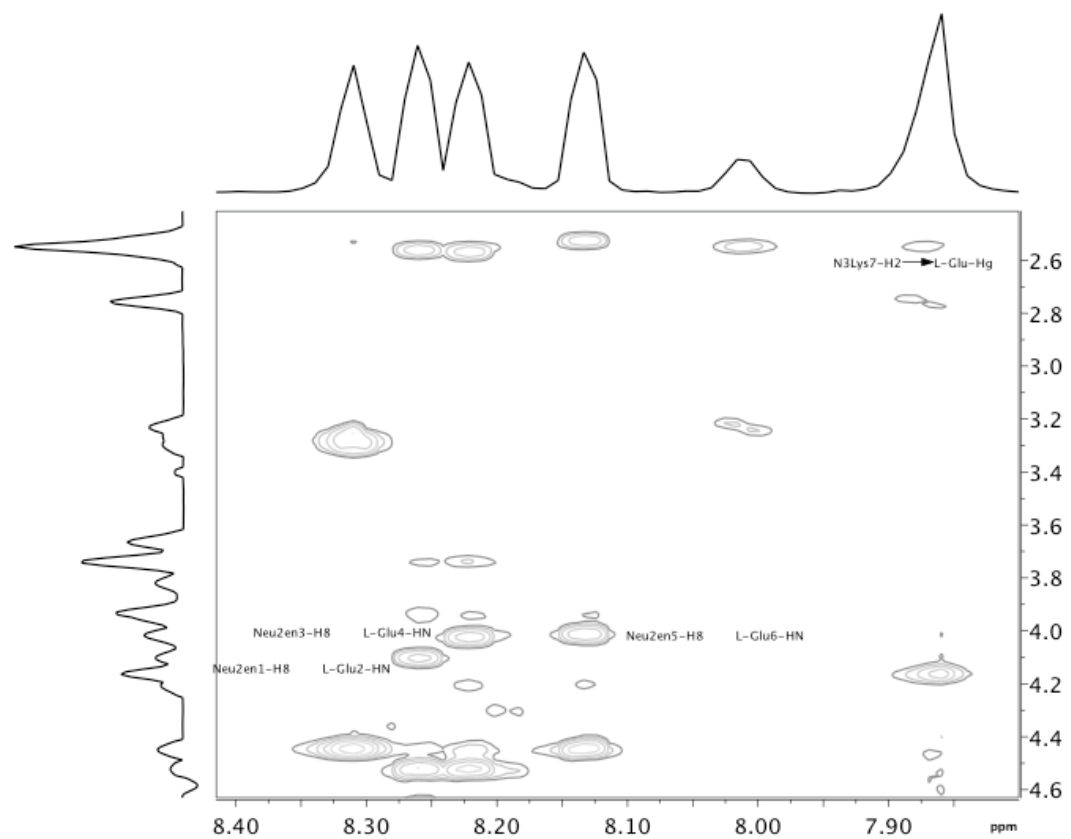


Figure S21. Prominent long range ROE's for **12**.

Figure S22. The effect of solvent and solvent screening of electrostatic charges in the X-PLOR structure calculation was implemented using the 1/R dielectric option for the electrostatic energy function in XPLOR by setting the dielectric constant equal to $\epsilon_0 R$. The electrostatic energy function ($f_{ELEC}(R)$) is given by:

$$f_{ELEC}(R) = Q_i Q_j \frac{C}{\epsilon_0 R^2} SW(R, R_{on}, R_{off})$$

where $SW(R, R_{on}, R_{off}) = 0$ or 1 if $R > R_{off}$ (7.5 Å) or $R < R_{on}$ (6.5 Å) respectively, and

$$SW(R, R_{on}, R_{off}) = \frac{(R^2 - R_{off}^2) (R^2 - R_{off}^2 + 3(R^2 - R_{on}^2))}{R_{off}^2 - R_{on}^2} \quad \text{if } R_{off} > R > R_{on}.$$

Table 1. Strong (s)^a, medium (m)^a and weak (w)^a ROEs observed in the 500 ms ROESY spectrum of **10** in 9:1 H₂O/D₂O at 600 MHz, 298 K.

Atom	Residue	Atom	Residue	ROE	Atom	Residue	Atom	Residue	ROE
α	1	γ	1	w	NH	4	5	4	w
α	1	β	1	w	NH	4	6	4	s
γ	1	β	1	w	NH	4	9	4	w
3	2	4	2	m	α	5	γ	5	w
3	2	α	3	w	γ	5	β	5	w
3	2	5	2	w	NH	5	α	3	w
4	2	5	2	w	NH	5	α	5	w
5	2	7	2	w	NH	5	β	5	w
6	2	β	1	w	NH	5	γ	5	w
6	2	9	4	w	NH	5	6	4 ^b	w
8	2	9	2	s	NH	5	7	4	w
9'	2	7	2	s	NH	5	9	4	w
NH	2	α	1 ^b	s	3	6	α	7	w
NH	2	α	3	w	3	6	4	6	m
NH	2	β	1	w	3	6	5	6	w
NH	2	4	2	w	5	6	9	6	w
NH	2	5	2	w	5	6	9'	6	w
NH	2	6	4	w	6	6	6	9	w
NH	2	9	2	w	8	6	9	6	s
α	3	γ	3	w	NH	6	α	5 ^b	s
α	3	9'	4	w	NH	6	4	6	m
γ	3	β	3	w	NH	6	5	6	w
NH	3	α	3	w	NH	6	6	6	s
NH	3	β	3	w	α	7	γ	7	w
NH	3	γ	3	w	α	7	8	6	w
NH	3	3	4	w	α	7	9'	6	w
NH	3	6	2 ^b	w	β	7	α	7	w
NH	3	7	2	w	β	7	δ	7	w
NH	3	8	2	w	δ	7	5	6	w
NH	3	9'	2	w	ε	7	δ	7	w
3	4	4	4	m	ε	7	γ	7	w
3	4	5	4	w	NH	7	α	7	w
3	4	9	6	w	NH	7	δ	7	w
3	4	9'	6	w	NH	7	γ	7	w
4	4	6	4	w	NH	7	ε	7	w
6	4	9	4	w	NH	7	3	6	w
8	4	α	3	w	NH	7	6	6	w
8	4	9	4	w	NH	7	7	6	w
9b	4	7	4	s	NH	7	8	6	w
NH	4	α	3 ^b	s	NH	7	9	6	w
NH	4	4	4	m	NH	7	9'	6	w

^aDistance were categorized s (2.9 Å), m (3.3 Å), and w (5.0 Å) as upper bond distance limits.

^bInterresidue ROE assignment consistent with calculations but ambiguous due to overlap.

Table 2. Strong (s)^a, medium (m)^a and weak (w)^a ROEs observed in the 500 ms ROESY spectrum of **12** in 9:1 H₂O/D₂O at 600 MHz, 298 K.

Atom	Residue	Atom	Residue	ROE	Atom	Residue	Atom	Residue	ROE
3	1	4	1	s	NH	4	γ	4	w
3	1	5	1	w	NH	4	3	3	w
3	1	9	3 ^b	w	NH	4	5	3	w
4	1	5	1	w	NH	4	6	3	w
6	1	8	1	w	NH	4	8	3	w
8	1	9	1	w	NH	4	9	5	w
9a	1	9'	1	m	NH	4	9'	5	w
9b	1	7	3	m	3	5	α	6	w
α	2	γ	2	w	3	5	4	5	s
α	2	β	2	w	3	5	5	5	w
NH	2	β	2	w	4	5	6	5	w
NH	2	γ	2	w	5	5	7	5	w
NH	2	3	1	w	6	5	7	5	w
NH	2	6	1	w	7	5	9'	5	s
NH	2	6	3	w	8	5	7	5	w
NH	2	8	1	w	NH	5	α	4 ^b	s
NH	2	9	3	w	NH	5	β	6 ^b	w
NH	2	9'	3	w	NH	5	4	5	m
3	3	4	3	s	NH	5	6	5	w
3	3	5	3	w	NH	5	7	5	w
3	3	5	5	w	α	6	β	6	w
3	3	6	5	w	α	6	γ	6	w
3	3	9	5 ^b	w	NH	6	β	6	w
4	3	6	3	w	NH	6	γ	6	w
6	3	7	5	w	NH	6	3	5	w
6	3	8	3	w	NH	6	5	5	w
7	3	9'	3	s	NH	6	6	5	w
NH	3	α	2 ^b	s	NH	6	8	5	w
NH	3	β	4 ^b	w	α	7	β	7	w
NH	3	4	3	m	α	7	γ	7	w
NH	3	6	3	w	α	7	δ	7	w
NH	3	7	3	w	β	7	γ	7	w
NH	3	9	5	w	γ	7	δ	7	w
α	4	β	4	w	NH	7	α	6	w
α	4	γ	4	w	NH	7	ε	7	w
NH	4	α	2	w	NH	7	NH	6	w
NH	4	α	4	w	NH ₂	7	α	7	w
NH	4	β	4	w	NH ₂	7	γ	4	w

^aDistance were categorized s (2.9 Å), m (3.3 Å), and w (5.0 Å) as upper bond distance limits.

^bInterresidue ROE assignment consistent with calculations but ambiguous due to overlap.

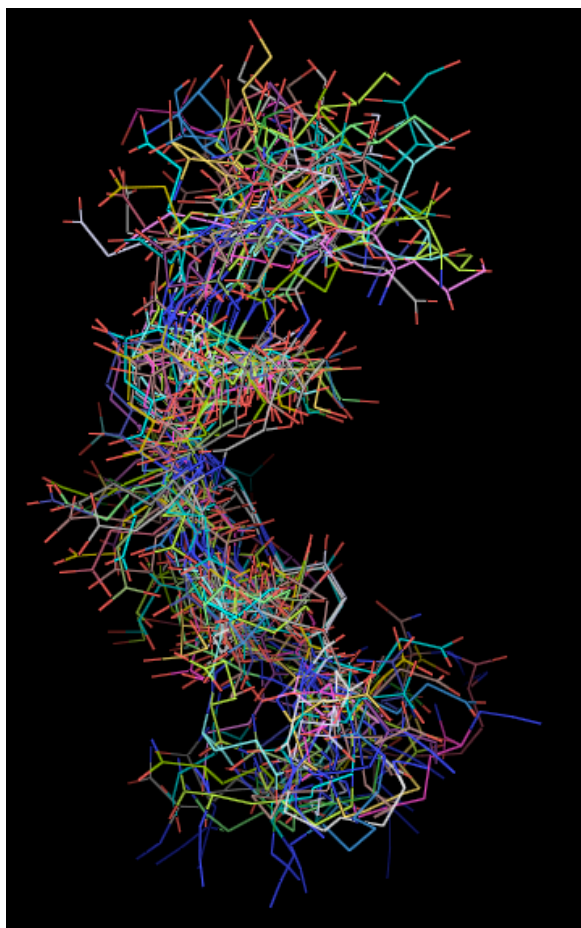


Figure S23. Overlay of 25 low energy structures of **8** showing non-convergence to a single-preferred structure; all H have been omitted for clarity (backbone atom rmsd: 2.080 ± 0.750 ; non-hydrogen atom rmsd: 3.325 ± 1.013).

Sample Name : Cpd 6
Solvent Name : D2O
Concentration : 0.36
Unit : mM

Function : Absorbance
Wavelength Range : 194 to 600 nm
Integration Time : 5.0 s

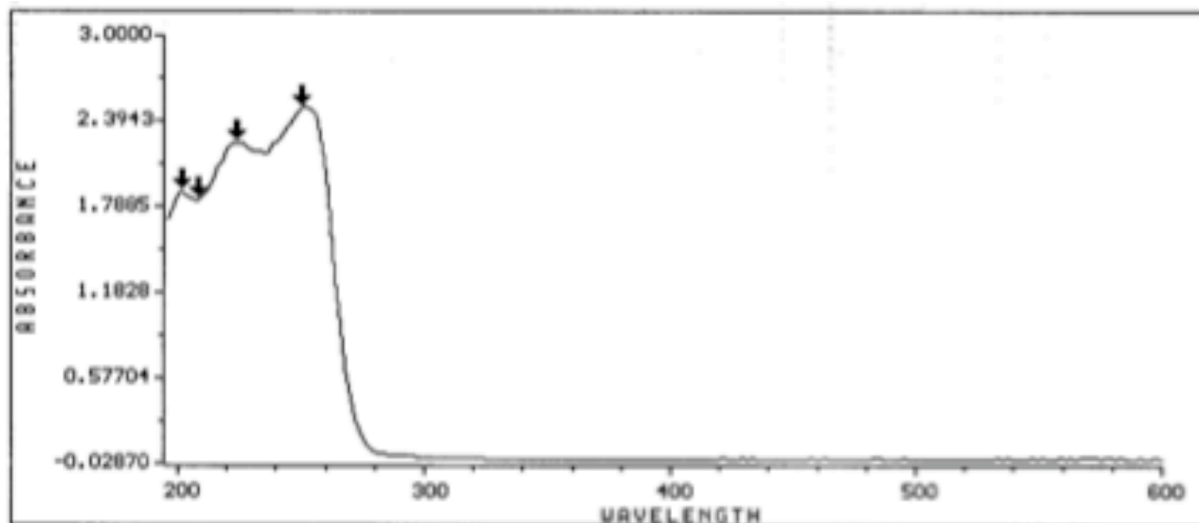


Figure S24. UV spectrum of 6 in D₂O.

Sample Name : Cpd 8
Solvent Name : D2O
Concentration : 0.36
Unit : mM

Function : Absorbance
Wavelength Range : 194 to 600 nm
Integration Time : 5.0 s

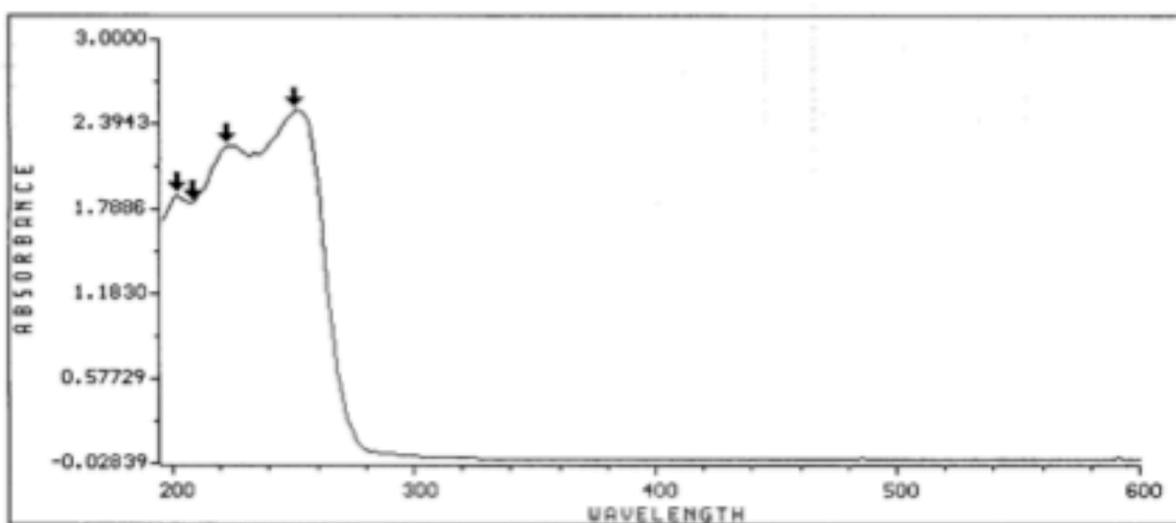


Figure S25. UV spectrum of 8 in D₂O.

Sample Name : Cpd **10**
Solvent Name : D2O
Concentration : 0.36
Unit : mM

Function : Absorbance
Wavelength Range : 194 to 600 nm
Integration Time : 5.0 s

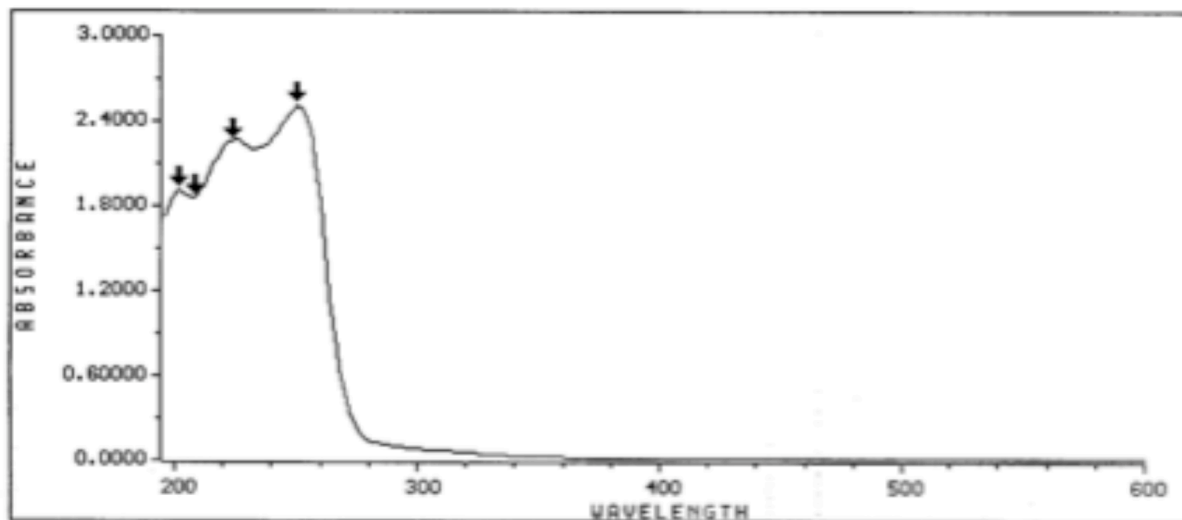


Figure S26. UV spectrum of **10** in D₂O.

Sample Name : Cpd **12**
Solvent Name : D2O
Concentration : 0.36
Unit : mM

Function : Absorbance
Wavelength Range : 194 to 600 nm
Integration Time : 5.0 s

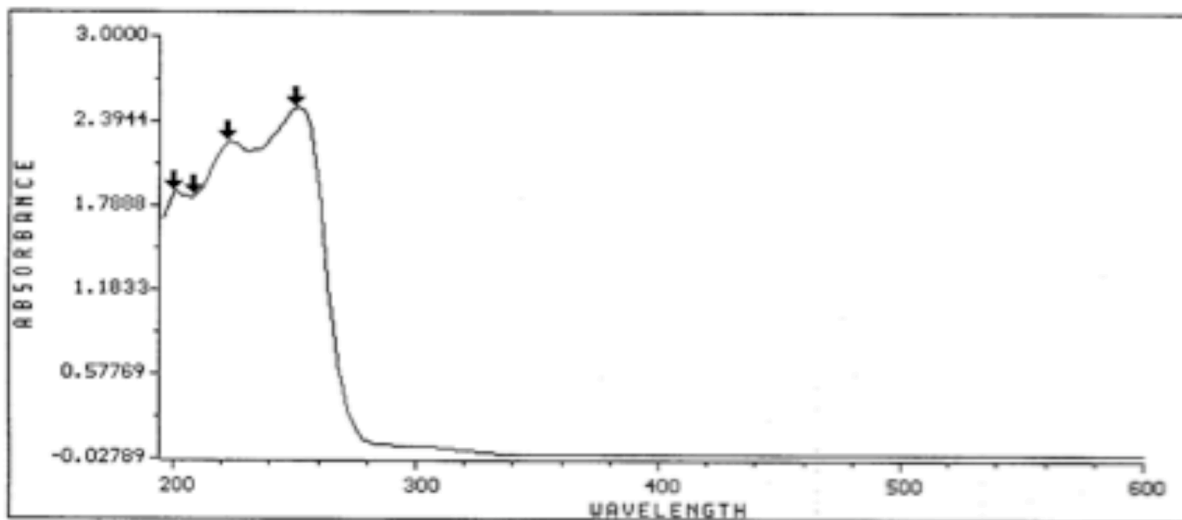


Figure S27. UV spectrum of **12** in D₂O.

References:

- (1) Gregar, T. Q.; Gervay-Hague, J. *J. Org. Chem.* **2004**, *69*, 1001-1009.
- (2) Nyffeler, P. T.; Liang, C.-H.; Koeller, K. M.; Wong, C.-H. *J. Am. Chem. Soc.* **2002**, *124*, 10773-10778.
- (3) Lundquist, J. T.; Pelletier, J. C. *Org. Lett.* **2001**, *3*, 781-783.